Research Paper

THEMED ISSUE: Different Personalities of Granites and Rhyolites: Silicic Magmas from the Lower Crust to the Surface

GEOSPHERE

GEOSPHERE, v. 19, no. 1

https://doi.org/10.1130/GES02438.1

7 figures; 2 tables; 1 set of supplemental files

CORRESPONDENCE: geokeith39@gmail.com

CITATION: Howard, K.A., Shaw, S.E., and Allen, C.M., 2023, Magmatic record of changing Cordilleran plate-boundary conditions—Insights from Lu-Hf isotopes in the Mojave Desert: Geosphere, v. 19, no. 1, p. 1–18, https://doi.org/10.1130/GES02438.1.

Science Editor: Shanaka de Silva
Guest Associate Editor: Jonathan S. Miller

Received 23 March 2021
Revision received 8 July 2022
Accepted 12 October 2022

Published online 5 January 2023

Magmatic record of changing Cordilleran plate-boundary conditions—Insights from Lu-Hf isotopes in the Mojave Desert

Keith A. Howard[1,*], Stirling E. Shaw[2,†], and Charlotte M. Allen[3,*]

[1]Scientist Emeritus, U.S. Geological Survey, Moffett Field, California 94035, USA
[2]Department of Earth and Planetary Sciences, Macquarie University, NSW 2109, Australia
[3]Department of Earth, Environmental, and Biological Sciences, Queensland University of Technology, 2 George St., Brisbane QLD 4000, Australia

ABSTRACT

Belts of Cordilleran arc plutons in the eastern part of the Mojave crustal province, inboard from the southwestern North American plate boundary, record major magmatic pulses at ca. 180–160 and 75 Ma and smaller pulses at ca. 100 and 20 Ma. This cyclic magmatism likely reflects evolving plate-margin processes. Zircon Lu-Hf isotopic characteristics and inherited zircons for different-age plutons may relate magma sources to evolving tectonics. Sources similar in age to the bulk of the exposed Mojave crust (1.6–1.8 Ga) dominated the magmas. Rare zircons having $\varepsilon Hf_{(t)}$ values as low as –52 indicate that Cretaceous melt sources also included more ancient crustal components, such as Archean-derived detritus in supracrustal gneisses of the Vishnu basin. Some rocks signal contributions from mantle lithosphere (in the Miocene) or asthenosphere (middle Cretaceous).

Temporal shifts in isotopic pattern in this sample of the Cordillera relate to cyclic pulses of magmatic flux. Hf-isotopic pull-downs suggestive of dominantly crustal sources characterize the Jurassic and Late Cretaceous flare-ups. The Late Cretaceous flare-up, occurring near the onset of flat-slab subduction, produced abundant Proterozoic xenocrystic zircon and Hf isotopes implicating derivation largely from heterogeneous deep Mojave crust. Isotopic pull-ups characterize the lower-flux middle Cretaceous and Miocene magmatic episodes. The middle Cretaceous pulse ca. 105–95 Ma produced Mojave crust signals but also the isotopically most juvenile magmatic zircons, ranging upward to barely positive εHf values and suspected to signal an asthenosphere contribution. This may point toward transtension or slab retreat causing 105–95 Ma backarc extension in the Mojave hinterland of the Cordillera. That possibility of backarc extension raises questions about the tectonic environment of the contemporaneous main Sierra Nevada high-flux arc closer to the continental margin.

INTRODUCTION

Magmatic arcs typically vary through time in their flux and isotopic character, commonly in cyclical patterns (Chapman and Ducea, 2019). The secular patterns offer opportunities to explore tectonomagmatic models (DeCelles et al., 2009; Kemp et al., 2009). For example, isotopic signatures can guide interpretation of contractional or extensional phases of subduction, on the premise that crustal thickening leads to more crustal magmatic signatures, whereas thinning leads to more mantle-like signatures (Kemp et al., 2009; Nelson and Cottle, 2018; Poole et al., 2020). Secular isotopic variations commonly relate to arc migration to different geographic positions, which obscures whether temporal changes reflect geographically different sources or else temporal changes such as in melt fertility (Chapman and Ducea, 2019). Documenting temporal changes in orogenic magmatism within a geographically restricted area could provide more clarity.

Southwestern North America provides a good environment to compare and track conditions of plate-margin magmatism related to changing active margin processes (Chapman et al., 2015, 2018; Profeta et al., 2015; Wooden et al., 2017a). The age contrast between Phanerozoic plutons and much older North American Precambrian crust they intrude in the Mojave Desert offers isotopic leverage for exploiting the plutons as probes of the crust and mantle and for exploring melt sources and compositional patterns (Wooden et al., 1988; Miller and Wooden, 1994; Barth and Wooden, 2010). Subduction at this part of the North American margin operated from ca. 250–20 Ma, during which the tectonism remains incompletely understood even though it is known that convergence varied in rate and sense of obliquity, and deformation in the orogen varied between contraction and extension (e.g., Ward, 1991; Walker et al., 2002). A succession of Phanerozoic magmatic episodes having arc-like geochemistry offers opportunities to plumb changing tectonomagmatic conditions. Their sundry arc-like compositions presumably reflect varied melt-fertile source regions. Zircon Lu-Hf isotopic character can offer insights into the variable interactions of magmas with Precambrian crustal elements and other possible components.

This paper uses U-Pb and Lu-Hf isotopic systematics to examine the evolution of Phanerozoic magmatism that periodically invaded the Precambrian Mojave crustal province. The magmatic episodes reflect evolving Mesozoic subduction conditions, followed by a Neogene transition from convergence to transform-fault tectonics

Keith A. Howard https://orcid.org/0000-0002-6462-2947
*E-mail: khoward@usgs.gov; cm.allen@qut.edu.au
†Deceased; 1933–2013

(Engebretson et al., 1984; Atwater and Stock, 1998). Single-grain zircon U-Pb ages and Hf isotopic ratios allow an exploration of magmatic sources and inferences on changing tectonic conditions for magmatic episodes spanning 150 million years from the Jurassic to the Miocene. The results show a cyclic pattern of increased crustal contributions during higher-flux magmatism compared to lower-flux episodes. In addition, the middle Cretaceous magmatism here on this inboard side of the orogen offers possible fresh insight to the tectonic environment during contemporaneous emplacement of the outboard Sierra Nevada and Peninsular Ranges batholiths (Fig. 1).

GEOLOGIC SETTING

Plate interactions between North America and oceanic plates to the west have shaped the evolution of the Cordilleran orogen and its continental magmatic arcs. The Phanerozoic magmatic record displays temporal compositional changes. For example, varying εHf and εNd reflect variable source contributions, $\delta^{18}O$ indicates variations in sedimentary source component, and Sr/Y and La/Yb act as proxies for fluctuating crustal thickness (Chapman et al., 2015, 2018; Profeta et al., 2015). Wooden et al. (2017a) reported preliminary results of secular changes in Hf isotopes from a broad regional study of the southwestern United States. The temporal variations relate partly to geographic distance from the plate boundary (Chapman and Ducea, 2019), varying systematically with eastward distance from the continental margin (Chapman et al., 2018). In contrast to these broad regional studies, our study allows a tight focus on the secular evolution, by examining plutons intruded from the Jurassic to the Miocene in a specific part of the hinterland, in continental crust hundreds of kilometers inboard of the modern and Mesozoic plate boundaries (Fig. 2).

Mojave Continental Crust

The Mojave crustal province (Fig. 1) of the North American craton was constructed and modified over several hundred million years in Proterozoic time and contains vestiges of Archean inheritance. Major crustal construction ca. 1.8–1.64 Ga produced plutons and orthogneisses that account for about two-thirds of the exposed Precambrian basement rocks (Wooden et al., 1988, 2013; Wooden and Miller, 1990; DePaolo et al., 1991; Anderson et al., 1992; Bender et al., 1993; Bryant et al., 2001; Barth et al., 2009; Holland et al., 2018). Crustal model ages (Nd, Hf, and Pb) generally are ca. 2.7–1.7 Ga (Fig. 1; Bennett and DePaolo, 1987; Wooden et al., 1988, 2013; DePaolo et al., 1991; Rämö and Calzia, 1998; Goodge and Vervoort, 2006). Diverse values of εHf in zircons in the orthogneisses and granitoids imply Precambrian contributions from juvenile components variably mixed with older components such as exposed supracrustal gneisses, some of which carry detrital early Paleoproterozoic and Archean zircons (Wooden et al., 2013; Holland et al., 2018). Mesoproterozoic ca.1.4 Ga granitoid plutons and small-volume ca. 1.1 Ga diabase sheets account for the final 10%–20% of the exposed Precambrian crust (Anderson and Bender, 1989; Hammond, 1990; Goodge and Vervoort, 2006; Wooden et al., 2013). Diverse zircon εHf values from the 1.4 Ga granitoids reflect the range of values observed in their 1.8–1.64 Ga host rocks and were interpreted to indicate derivation primarily from anatexis of preexisting Mojave crust (Goodge and Vervoort, 2006) and perhaps also some enriched lithospheric mantle (Wooden et al., 2013). The crust in our eastern Mojave study area (Fig. 2) differs in subtle to overt ways from the Yavapai crustal province on the east (Fig. 1) as well as from adjacent Mojave areas to the west, northwest, south, and southwest (Bennett and DePaolo, 1987; Tosdal et al., 1989; DeWitt, 1991; Anderson et al., 1992; Miller and Glazner, 1995; Miller et al., 2000; Wooden and Bryant et al., 2001; Rämö et al., 2002; Tosdal and Wooden, 2015; Chapman et al., 2018).

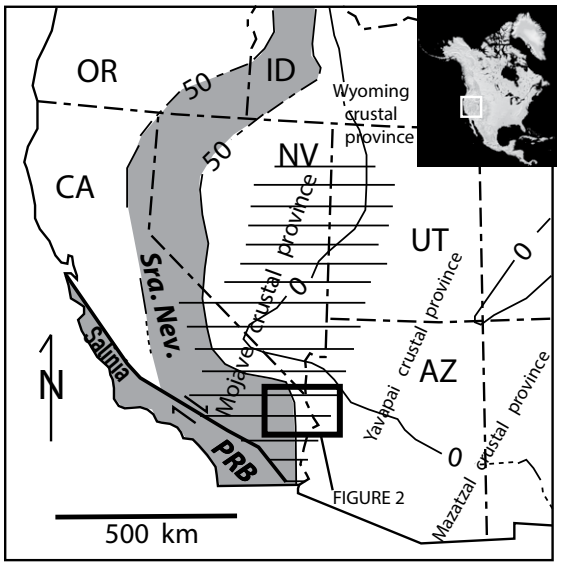

Figure 1. Map of southwestern United States showing the eastern Mojave Desert study area (box) in relation to the Sierra Nevada (Sra. Nev.) and Peninsular Ranges (PRB) batholiths and magmatic arcs. Contours are shown for 50% and (east of the main arc) 0% of Mesozoic (and minor Paleogene) plutonic rocks relative to their host rocks (after Miller and Barton, 1990). Mojave (horizontal lines) and some other North American crustal provinces indicated. Inset shows position in North America.

Subcrustal Lithosphere

Numerous studies have concluded that an enriched ancient mantle lithosphere lies below the eastern Mojave province crust (e.g., Farmer et al., 1989; Miller et al., 2000; Ryan, 2011). Mantle xenoliths in late Cenozoic basalts in the eastern Mojave Desert include Paleoproterozoic to possible Neoarchean mantle components (Lee et al., 2001),

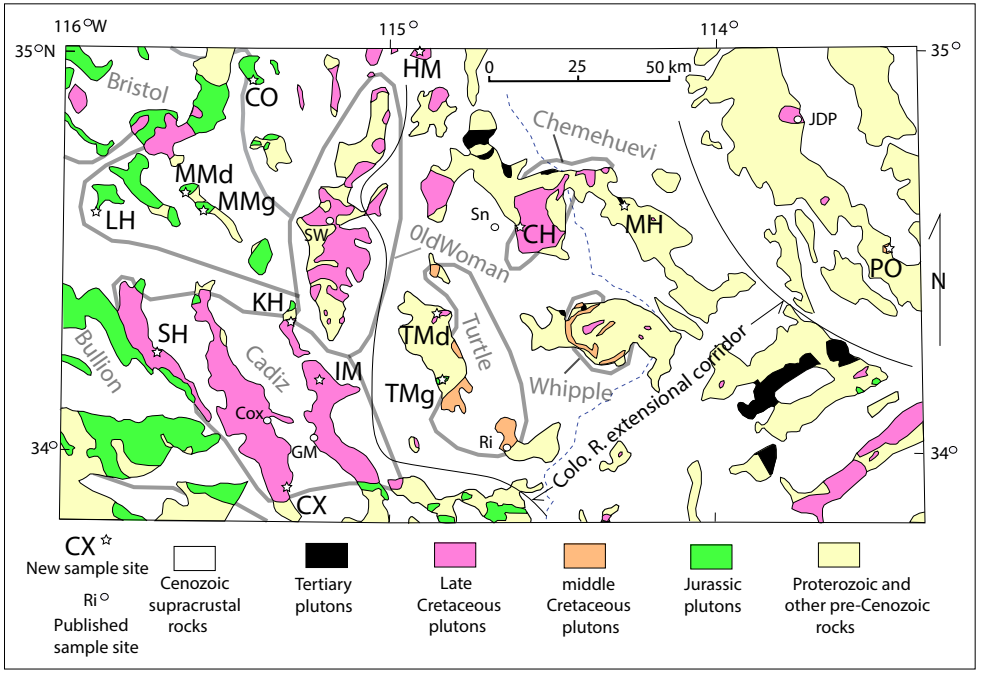

Figure 2. Geologic map of the eastern Mojave Desert study area showing Hf sample sites (Table 2). Batholiths and intrusive sequences outlined by gray lines are the Jurassic Bristol (Bristol Mountains sequence; Barth et al., 2017) and Bullion (Bullion Mountains Intrusive Suite); the middle Cretaceous Whipple (Whipple Wash suite; Anderson and Cullers, 1990) and Turtle (Turtle assemblage); and the Late Cretaceous Cadiz (Cadiz Valley), Old Woman (Old Woman–Piute), and Chemehuevi (Chemehuevi Mountains) batholiths. Miocene Colorado River (Colo. R.) extensional corridor is indicated. Colorado River (dashed line) bounds California (left) from Arizona. Mapping by the authors.

and late Cenozoic basalts show isotopic evidence of contributions from mantle lithosphere (DePaolo, 1992; Bradshaw et al., 1993; Daley and Feuerbach et al., 1993; Miller et al., 2000; McDowell et al., 2016). Mantle lithosphere components could include pyroxenite veins, garnet pyroxenites as arclogite residue of Mesozoic granitoid generation, or even ancient sediments structurally incorporated into a mantle keel (Beard and Johnson, 1997; Chapman et al., 2020). Mesozoic and Cenozoic tectonism likely shuffled or translocated subcrustal mantle lithosphere provinces beneath the region (Feuerbach et al., 1998; Luffi et al., 2009), with Late Cretaceous–Paleogene flat-slab subduction removing ancient lithosphere west of the study area judging from isotopic signals in Cenozoic basalts (Miller et al., 2000; Luffi et al., 2009; Chapman et al., 2018, 2020). Evidence that flat-slab subduction underplated and likely displaced or shuffled ancient lithosphere includes underplated Orocopia Schist exposed west and southeast of the study area (e.g., Strickland et al., 2018) and xenoliths on the Colorado Plateau thought to record eastward-underthrust deep arclogite displaced from the Mojave area where it had formed the residue of Mesozoic granite generation (Chapman et al., 2020).

Mesozoic and Cenozoic Magmatism

Mesozoic and Cenozoic plate-boundary tectonism and magmatism in the eastern Mojave region followed hundreds of millions of years of cratonic stability, recorded by thin Paleozoic marine shelf sequences deposited on the Proterozoic basement. After Permian-to-Triassic continental truncation exposed this part of the former craton to active-margin tectonics (Hamilton, 1969), subduction processes constructed Mesozoic magmatic arcs starting ca. 250 Ma along the western part of North America, at this latitude extending far eastward into the old cratonic basement (Fig. 1; Burchfiel and Davis, 1975, 1981; Chapman et al., 2015; Barth et al., 2017). Mesozoic orogenic fluctuations in crustal thickness, still incompletely understood, led eventually to denudation of plutonic parts of the Mesozoic arcs, followed in the early Miocene by renewed magmatism, extensional crustal thinning, and formation of metamorphic core complexes. How the magmatic successions related specifically to tectonics is imperfectly understood but may have included complex interactions involving sinking of eclogite roots (DeCelles et al., 2009) and/or subduction-related tectonic mode switching between convergent contraction and/or other extension (Kemp et al., 2009).

The eastern Mojave area spans the inboard margins of major subduction-related Mesozoic magmatic arcs, where the Mesozoic plutonic fraction relative to older host rocks decreases eastward from >70% to <5% (Fig. 1). The 240-km-wide study area (Fig. 2) was an estimated 25% narrower east-west before the Neogene if retrodeformed to restore extension and dextral shearing (Howard and John, 1987; Howard, 2002; Bennett et al., 2016). Jurassic and Late Cretaceous plutons underlie much of the western part of the area (Fig. 2). They reflect relatively high-flux Jurassic and Late Cretaceous magmatic flare-ups of limited duration. Less extensively exposed middle Cretaceous and Miocene plutonic rocks in the study area record two short, smaller magmatic pulses, which we characterize as lower-flux events. Table 1 summarizes some characteristics of the episodes. An earlier onset of arc magmatism focused Permian to Triassic plutonism west of the eastern Mojave study area (Barth et al., 1997; Cecil et al., 2019).

Jurassic plutons in the study area (Fig. 2) form part of a ca. 180–160 Ma magmatic arc extending

TABLE 1. CHARACTERISTICS OF PLUTONS IN THE EASTERN MOJAVE DESERT

Emplacement age	(Ma)	Petrology	$^{87}Sr/^{86}Sr_i$	$\varepsilon Nd_{(t)}$	Isotope references
Early Miocene	21–18; one 26	High-K calc-alkaline, metaluminous, compositionally expanded gabbro to granite. Mesozonal to epizonal with volcanic cover.	0.708–0.712	–5 to –10	Miller et al. (2000); McDowell et al. (2016)
Late Cretaceous	85–65	High-K calc-alkaline, mostly granite and granodiorite. Metaluminous to highly peraluminous. Mesozonal.	0.707–0.713	–8 to –18	Miller et al. (1990); Phillips et al., (2014); Fisher et al. (2017)
Middle Cretaceous	110–90	Calcic to calc-alkaline, metaluminous to peraluminous. Mostly granodiorite. Mesozonal to epizonal.	0.705–0.710	–3 to –8	Allen et al. (1995)
*Late Jurassic	155–145	Sparse mafic to felsic dikes.	0.705–0.720	–13 to –16	Gerber et al. (1995)
Early Late Jurassic	164–161	Alkali-calcic, metaluminous. Compositionally expanded diorite to quartz monzonite to granite. Mesozonal to epizonal.	0.707–0.712	–8 to –18	Miller et al. (1990); Young et al. (1992); Gerber et al. (1995); Tosdal and Wooden (2015)
Late Middle Jurassic	176–164	Metaluminous, high-K calc-alkaline diorite to quartz monzonite and granite. Mesozonal to epizonal with volcanic cover.	0.706–0.726	–4 to –12	Gerber et al. (1995); Tosdal and Wooden (2015)

*Small-volume dikes; no Hf data.

through east-central California southeast into Arizona and Mexico (Burchfiel and Davis, 1981; Tosdal et al., 1989; Tosdal and Wooden, 2015; Barth et al., 2017). Within the study area, this episode included a geochemical transition at ca. 164 Ma from high-K calc-alkalic plutonism (Middle Jurassic Fort Irwin and Bullion sequences) to shoshonitic light-rare-earth–enriched alkali-calcic plutonism (early Late Jurassic Bristol Mountains sequence; Barth et al., 2017). This latter sequence was suggested to record ponding of melt at deepening levels during crustal thickening (Barth et al., 2017). Alternatively, from structural evidence and trace-element geochemical proxies of crustal thickness, the Mojave crust may have been thinning during this time (Davis et al., 1994; Profeta et al., 2015). Younger low-volume Late Jurassic dikes and plutons, common farther west in the Mojave Desert, are locally present in the study area but were not sampled in our study.

Middle Cretaceous 105–95 Ma plutons in the study area form small outliers in a backarc position well inboard of the contemporaneous main middle Cretaceous arc formed by the Sierra Nevada and tectonically displaced Salinia and Peninsular Ranges batholiths (Fig. 1). The middle Cretaceous plutons in the study area (Fig. 2) are more calcic and less evolved in Sr isotopes than in voluminous neighboring Jurassic and Late Cretaceous plutons (Anderson and Cullers, 1990; Allen et al., 1995; Wooden et al., 2017b). The middle Cretaceous magmatism occurred during a time when thick continental sediments were accumulating nearby in the McCoy Mountains Formation basin, and the upper crust was shortening in the Maria fold and thrust belt adjacent to that basin and in the Sevier thrust belt in southern Nevada (Barth et al., 2004; Hildebrand and Whalen, 2017).

Younger voluminous Late Cretaceous calc-alkalic plutons ca. 85–65 Ma (Fig. 2) record part of an eastward sweep of magmatism commonly considered to mark the eastward progression of a shallowing subducting slab (Coney and Reynolds, 1977). The ca. 76–72 Ma Cadiz Valley and Old Woman–Piute batholiths contain abundant inherited Proterozoic zircon (Foster et al., 1989; Miller et al., 1992; Economos et al., 2010a, 2010c, 2021; Phillips et al. 2014). These xenocrysts and whole-rock Sr, Nd, Pb, and O isotopic characteristics point to considerable crustal contributions to the plutons (Table 1; Wooden et al., 1988; DePaolo et al., 1991; Miller and Wooden, 1994). The Old Woman–Piute batholith's zircon and monazite preserve wide ranges of Hf and Nd isotopic ratios reflecting Precambrian sources of the Mojave crustal province (Phillips et al., 2014; Fisher et al., 2017). The Late Cretaceous magmatism coincided with extensional faulting in the middle crust (Wells and Hoisch, 2008).

In the early Miocene, plutonism along the Colorado River extensional corridor (roughly 114°–115° west longitude in Fig. 2) produced scattered high-K calc-alkaline rocks of an expanded range of compositions (diorite, granodiorite, and granite) in concert with coeval volcanic rocks (Anderson and Cullers, 1990; Campbell-Stone et al., 2000; Bryant et al., 2001; Howard et al., 2013; McDowell et al., 2016). Arc-like compositions, despite an extensional post-subduction tectonic setting, invite comparison of this magmatic episode to the Mesozoic arcs. The plutons are mostly 21–18 Ma in the study area. Similar but slightly younger plutons and volcanic rocks just north of the study area show ranges in whole-rock and zircon $\varepsilon Hf_{(t)}$ values (e.g., –5 to –20 in plutonic zircon) consistent with hybrid magmas sourced from varied proportions of mantle and ancient crustal components (Miller et al., 2009; Ryan, 2011; McDowell et al., 2016). As extension and magmatism waned in the late Miocene, the magmatism transitioned to eruption of juvenile basalts (Bradshaw et al., 1993; Miller et al., 2000).

ZIRCON U-Pb AND Lu-Hf STUDY

Plutons Sampled

Fourteen plutons chosen to represent Middle Jurassic, Late Jurassic, middle Cretaceous, Late Cretaceous, and early Miocene magmatic episodes across the study area were sampled for single-crystal zircon analysis for U-Th-Pb age and Lu-Hf isotopes (Fig. 2; Table 2). Ten of the sampled plutons were previously undated by U-Pb. Granite to granodiorite compositions predominate, but three dioritic samples (Late Jurassic, Late Cretaceous, and Miocene) provide data on more mafic components. Additional information can be found in the Supplemental Material[1].

Two sampled Jurassic rocks, samples CO and TMg, fit in age and composition with Barth et al.'s (2017) high-K calc-alkalic Middle Jurassic sequences. The slightly younger Late Jurassic alkali-calcic Bristol Mountains sequence was sampled in three plutons (LH, MMg, and MMd). Middle Cretaceous granodiorite (PO), sampled near the eastern edge of the Mojave crustal province (Bryant et al., 2001; Goodge and Vervoort, 2006), resembles (in its alkali/lime ratio) calcic granodiorites of the middle Cretaceous Turtle assemblage (Allen et al., 1995). Late Cretaceous rocks were sampled at seven sites, three of them in the Cadiz Valley batholith (CX, SH, and IM), one in the Old Woman–Piute batholith (KI), one in the Chemehuevi Mountains batholith (CH), plus another granite (HM), and a quartz diorite (TMd). We sampled one early Miocene pluton, diorite (MH), which contains moderately high MgO (8.6%), Cr (472 ppm), and Ni (121 ppm) (Item 5, see footnote 1).

Zircon Morphology

Zircon samples were prepared at Macquarie University (Sydney, Australia), where zircons were

TABLE 2. ZIRCON SAMPLES AND SUMMARY U-Pb AGES

Pluton age	Zircon sample	Rock	SiO_2 (%)	Rock age[1]	Older Mesozoic ages present (Ma)	Concordia upper intercept (n) or spot Precambrian age (Ma[2])
				$^{206}Pb/^{238}U$ age Ma ± 2 s.d. (n)[3]		$^{207}Pb/^{235}U$ versus $^{206}Pb/^{238}U$ ± 2 s.d. (n)[3]
Miocene	MH	Diorite in Mohave Mountains	54	20.0 ± 0.4 (4)	N/A	N/A
Late Cretaceous	CH	Chemhuevi Peak Granodiorite	69	72 ± 2 (3)	140 (2)	1552 ± 19 (5)
	HM	Granite of Homer Mountains	73	72 ± 1 (6)	82, 164	1720 ± 28 (14)
	SH	Sheep Hole Mountains Granodiorite	68	73 ± 2 (10)	125	N/A
	KI	Old Woman Mountains Granodiorite	65	74 ± 1 (4)	N/A	N/A
	TMd	Quartz-bearing diorite, Turtle Mountains	61	73 ± 5 (10,D)	177	N/A
	CX	Granodiorite in Coxcomb Mountains	68	75 ± 3 (7, D)	188	1580 (1)
	IM	Danby Lake Granite Gneiss[4]	75	ca. 75	N/A	1475; 1700 (9)
Middle Cretaceous	PO	Granodiorite, Poachie Range	70	96 ± 3 (5)	100	1400; 1661 ± 28 (14,D)
Late Jurassic	LH	Quartz monzonite, Lava Hills	67	162 ± 3 (11,D)	168(?)	N/A
	MMd	Quartz diorite, Castle Mine, Marble Mountains	57	159 ± 4 (6,D)	175	N/A
	MMg	Granite of Iron Hat Mine, Marble Mountains	76	164 ± 5 (6)	170	N/A
Middle Jurassic	TMg	Granite of southern Turtle Mountains	70	168 ± 4 (9)	N/A	N/A
	CO	Granodiorite, Colton Hills	70	179 ± 11 (11,D)	192, 200	1615 ± 18

[1]Weighted-mean $^{206}Pb/^{238}U$ age or intercept age marked as "D." Uncertainties all quoted as 95% confidence with dispersion as generated in IsoplotR (Vermeesch, 2018).
[2]Upper intercept concordia age. N/A–not applicable.
[3]Parentheses indicate number of grains used for calculating mean age. s.d.—standard deviation.
[4]IM's pluton is constrained in age to 75.5 ± 2 Ma by intrusive relations with two plutons dated by Wells et al. (2002).

[1]Supplemental Material. Item 1: Sample descriptions and U-Pb age. Item 2: Zircon analytical procedures. Item 3: Lu-Hf isotope calculations. Item 4: Supplementary U-Pb age plots. Item 5: Whole-rock chemistry of samples. Item 6: U-Th-Pb isotopic analyses. Item 7: Lu-Hf isotopic analyses. Please visit https://doi.org/10.1130/GEOS.S.21528918 to access the supplemental material, and contact editing@geosociety.org with any questions.

separated from crushed rock powder by panning and hand picking (Item 2, see footnote 1). The zircon grains generally range in size from 100 to 150 microns. Aspect ratios vary from ~3:1–1:1. Grain habit is generally idiomorphic with dominant prism faces terminated by pyramids. Some irregularly shaped grains are interpreted as fragments of larger crystals. All zircons are zoned to some degree in cathodoluminescence images, varying from concentric, finely developed dark and light bands (Fig. 3A), through sets of truncated zones representing different growth stages (Fig. 3B), to a combination of regular finely zoned overgrowths about areas of irregularly shaped coarse patchy zones (Fig. 3C). In addition to complex zoning, many zircons have inherited cores, varying from irregular and rounded shapes (Figs. 3A) to microgranular aggregates (Fig. 3C). Irregular and patchy zones in some zircons may record metamorphic recrystallization. Previous study of zircon in the Old Woman–Piute batholith (Late Cretaceous) found very complex zoning, especially in strongly peraluminous granite, where some zircon zones were interpreted to record Proterozoic metamorphism (Miller et al., 1992).

Zircon Analysis

Single grains were analyzed at Macquarie University by S.E. Shaw by laser-ablation (LA) isotopic analysis first for U-Th-Pb by inductively coupled plasma mass spectrometry (ICPMS) and then for most of these dated grains in a separate laser spot for Lu-Hf using multi-collector ICPMS (LA-MC-ICPMS). The two laser spots were placed as symmetrically as possible relative to crystal shape and cathodoluminescence pattern (Fig. 3). The zircons are mostly complexly zoned (Fig. 3), and the laser-ablation spot sizes (30–55 μm) commonly sampled multiple crystal zones. We determined 264 U-Pb isotopic analyses and 159 Lu-Hf isotopic analyses (Items 6 and 7; see footnote 1).

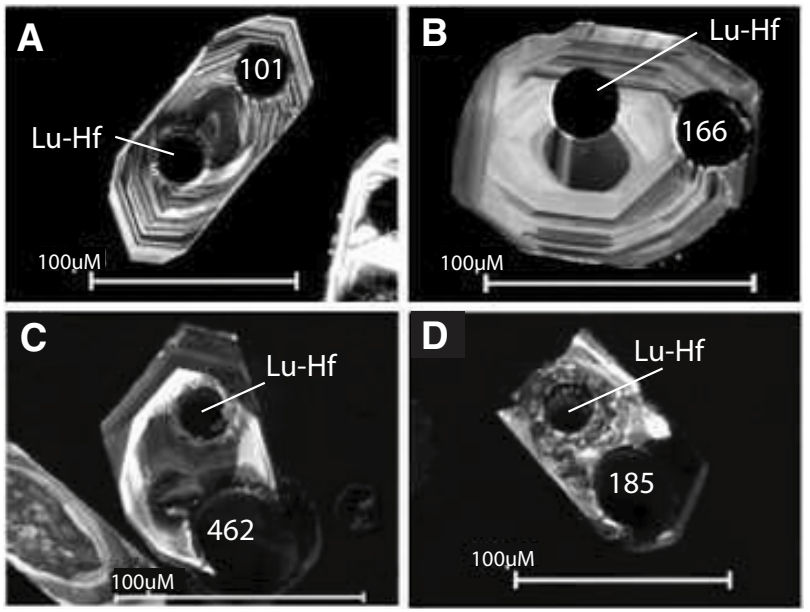

Figure 3. Examples of zircon cathodoluminescence images, showing larger U-Pb laser spot (apparent age in Ma) and the smaller Lu-Hf laser spot. (A) Middle Cretaceous rock PO, grain 12 (Hf model age 2500 Ma). (B) Jurassic rock MMd, grain 5 (Hf model age 1800 Ma). (C) Late Cretaceous rock IM, grain 8 (discordant U-Pb age; Hf model age would be Neoarchean). (D) Rock IM, grain 6 (the larger U-Pb laser spot partly sampled outer zones giving a composite discordant $^{206}Pb/^{238}U$ apparent age of 185 Ma; Hf model age of microgranular core would be Archean).

RESULTS

The U-Th-Pb dating provided age control for the Lu-Hf results and context for magmatic and inherited zircon as detailed in Items 1, 4, and 6 (see footnote 1) and summarized briefly here and in Table 2 and Figure 4.

U-Pb Pluton Ages

Table 2 lists generally a weighted-mean $^{206}Pb/^{238}U$ age of a concordant population as the intrusion age. The intrusion ages align with geological constraints. Concordance criteria are two times standard deviation (relaxed to four times standard deviation for the Miocene sample MH). Several samples show obvious zircon inheritance (Fig. 4). U-Pb concordia upper and/or lower intercept ages were calculated for some samples to describe both intrusion age and inheritance age (Table 2 and Items 1 and 4, see footnote 1). Complex crystal zoning, abundant evidence of common Pb, and exclusion of data outliers from age calculations introduce uncertainties that may exceed the calculated analytical age uncertainties. Discordant ages occur for about half of the analyses, likely owing to common lead and to laser spots sampling multiple crystal zones.

Samples CO and TMg yielded late Middle Jurassic magmatic intrusion ages akin to the calc-alkaline Fort Irwin and Bullion sequences (Barth et al., 2017). Sample CO exhibits five concordant U-Pb ages ranging 200–170 Ma (Item 4, see footnote 1). Samples MMd, MMg, and LH yielded magmatic ages ca. 164–159 Ma, consistent with other members of the mostly early Late Jurassic alkali-calcic Bristol Mountains sequence (Barth et al., 2017). These three Bristol Mountains sequence samples

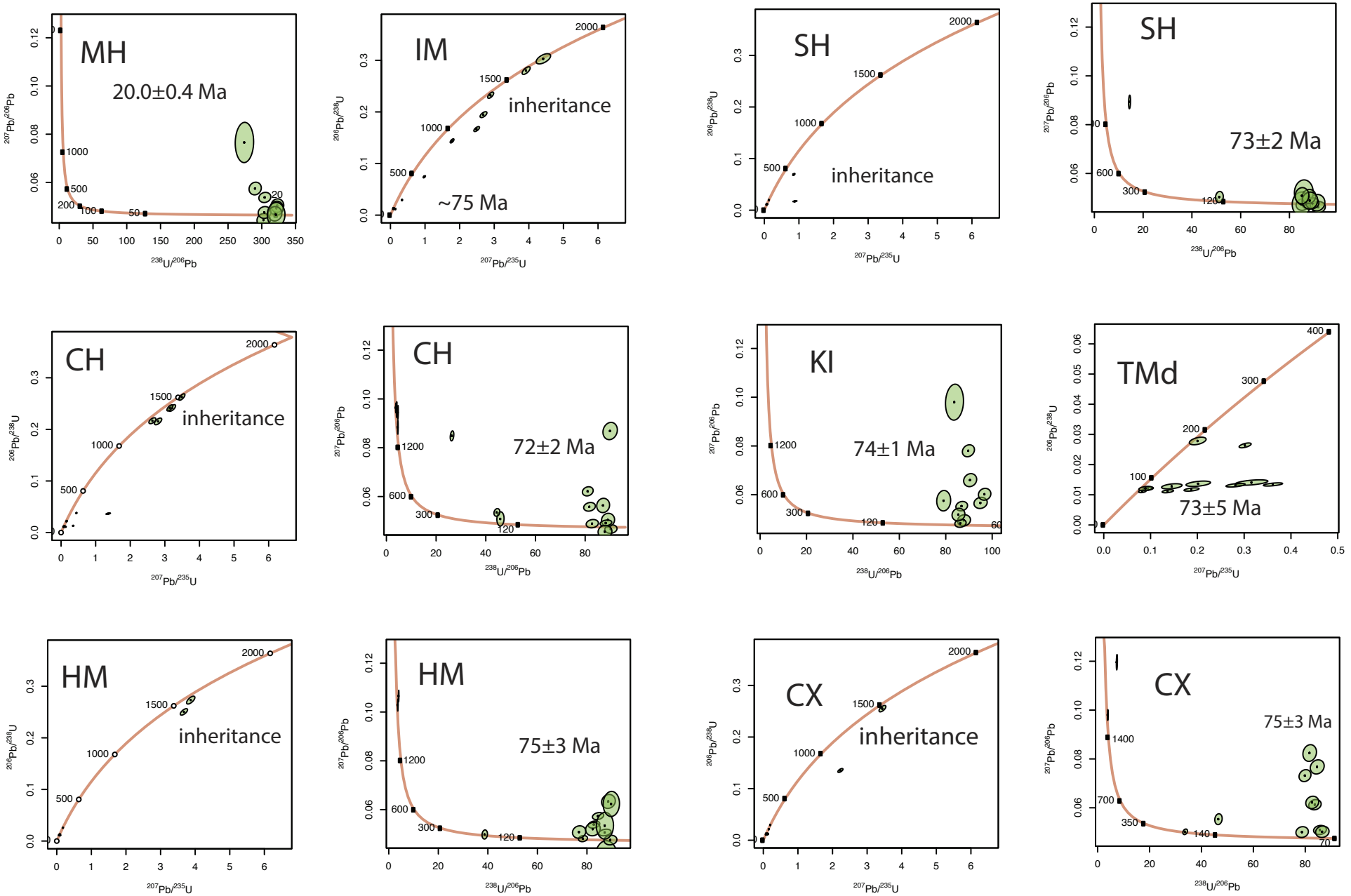

Figure 4. ***Continued on the following page.***

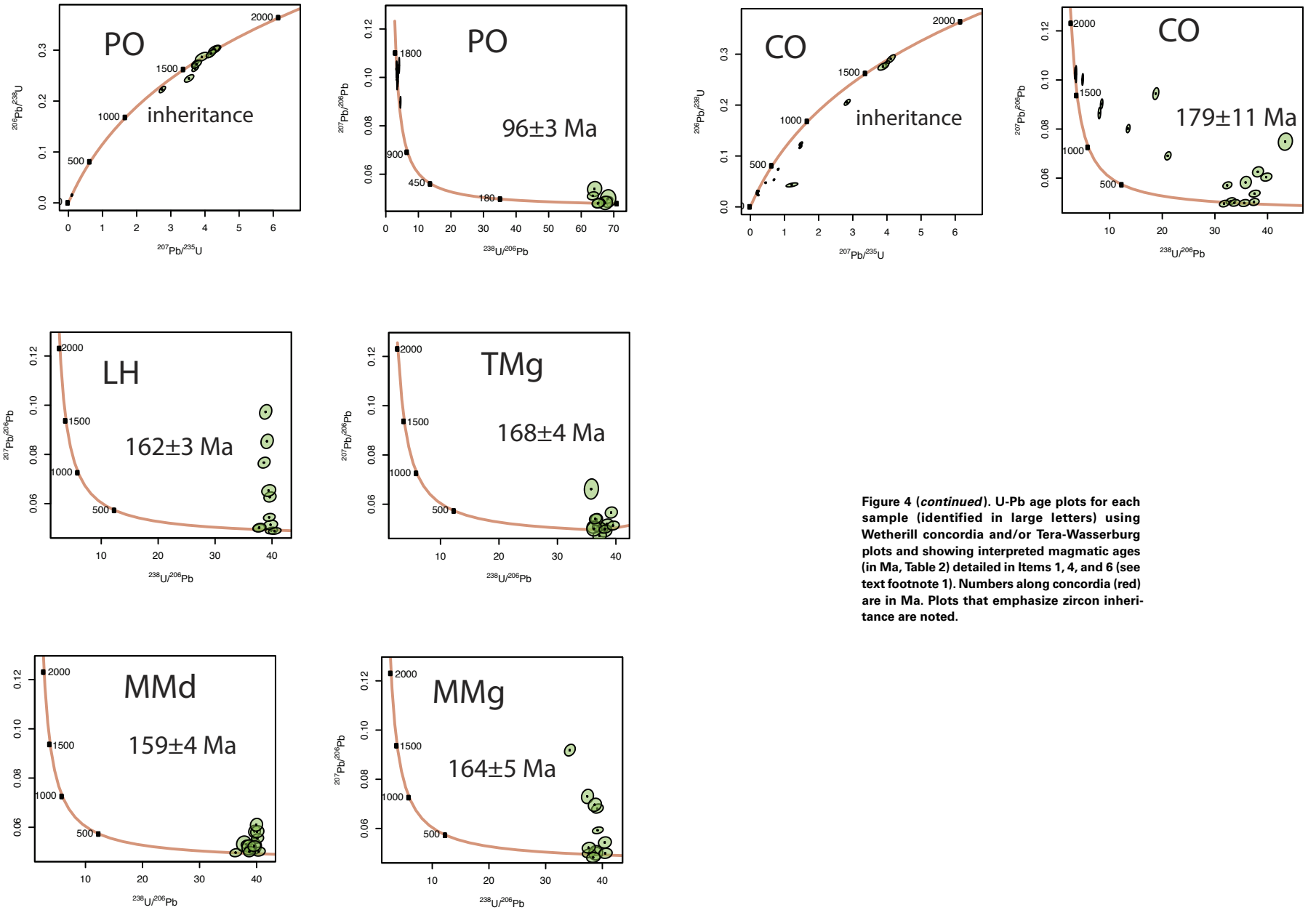

Figure 4 (*continued*). U-Pb age plots for each sample (identified in large letters) using Wetherill concordia and/or Tera-Wasserburg plots and showing interpreted magmatic ages (in Ma, Table 2) detailed in Items 1, 4, and 6 (see text footnote 1). Numbers along concordia (red) are in Ma. Plots that emphasize zircon inheritance are noted.

have strong common lead signals, with values of $^{207}Pb/^{206}Pb$ >1.

The magmatic age of sample PO, 96 ± 3 Ma, places it in the middle Cretaceous pluton group that includes the Turtle assemblage (Allen et al., 1995) and Whipple Wash suite (Anderson and Cullers, 1990; Wooden et al., 2017b). Seven samples have Late Cretaceous intrusion ages of ca. 76–72 Ma (Fig. 4), like many other lithologically similar other Late Cretaceous rocks in the area (Calzia et al., 1986; Wright et al., 1987; Foster et al., 1989; Kula et al., 2002; Wells et al., 2002; Barth et al., 2004, 2017; Economos et al., 2010a, 2021; Chapman et al., 2018).

Miocene diorite MH's mean U-Pb population age of 20.0 ± 0.4 Ma compares with Tertiary plutons in nearby ranges dated ca. 19–18 Ma, one dated ca. 26 Ma, and dike swarms dated ca. 22–18 Ma (John and Foster, 1993; Pease et al., 1999, 2005; Campbell-Stone et al., 2000; Howard et al., 2013; Gans and Gentry, 2016; LaForge et al., 2017; Wooden et al., 2017b).

Inherited Xenocrystic Zircon

Inherited zircon cores dated as Proterozoic by $^{207}Pb/^{206}Pb$ occur in Middle Jurassic, middle Cretaceous, and Late Cretaceous rock samples. Inherited Mesozoic zircon was found in Jurassic and Late Cretaceous samples.

Inherited Proterozoic zircon (Fig. 4) occurs in Middle Jurassic granodiorite CO as it does also in a previously analyzed Middle Jurassic granodiorite 15 km south of the CO site (Gerber et al., 1995; Howard et al., 1995; Barth et al., 2017), and in the compositionally similar Jurassic Kitt Peak–Trigo Mountains superunit southeast of the study area (Tosdal and Wooden, 2015). In the Late Jurassic Bristol Mountains sequence, we measured no inherited Precambrian zircon but some apparently premagmatic Middle Jurassic zircon.

Inherited Proterozoic zircon is common in the area's Cretaceous plutons (Wright et al., 1987; Foster et al., 1989; Allen et al., 1995; Economos et al., 2010b, 2021; Wooden et al., 2017b;). More than half of the dated zircons in the middle Cretaceous granodiorite (PO) are Proterozoic, indicating a weighted-mean $^{207}Pb/^{206}Pb$ age 1661 ± 28 Ma not counting a ca. 1400 Ma grain. Four of the seven sampled Late Cretaceous granitoids also contain inherited Proterozoic zircon, ranging from ca. 1730–1390 Ma but mostly ca. 1720–1630 Ma. Proterozoic inheritance dominates peraluminous Late Cretaceous granite gneiss IM, analogous to peraluminous granite in the nearby Late Cretaceous Old Woman–Piute batholith (Miller et al., 1992).

The Late Cretaceous rocks yielded six concordant pre-pluton Cretaceous and Jurassic xenocrysts in addition to the Proterozoic inheritance. Three Late Cretaceous rocks (CH, HM, and TMd) contain Jurassic zircon even though they occur northeast of the exposed belt of Jurassic plutons (Jurassic zircon xenocrysts northeast of the exposed Jurassic pluton belt are also present in Cretaceous plutons in the Whipple Mountains and in a ca. 66 Ma pluton 60 km north of the study area (Kapp et al., 2002; Gans and Gentry, 2016). Abundant xenocrystic zircon in Cretaceous plutons and in Middle Jurassic rock CO is consistent with magmas that were generally <800 °C, saturated in zircon, derived at least partly from zircon-bearing source rocks of the Mojave province, and likely associated with an influx of fluid (Miller et al., 2003).

Miocene diorite (MH) yielded no clearly inherited zircon, like some other Miocene intrusions in the area of Figure 2 (Howard et al., 2013). Others exhibit Proterozoic inheritance (Pease et al., 1999; Bryant and Wooden, 2008; Gans and Gentry, 2016).

Lu-Hf Isotopic Results

A hafnium isotope evolution diagram displays age-corrected (t) εHf data that correspond to our U-Pb ages that are concordant (83 out of 159 analyses) in $^{206}Pb/^{238}U$ age (or $^{207}Pb/^{206}Pb$ for Precambrian grains) (Fig. 5). Plotting age-corrected εHf results for only concordantly dated grains minimizes the problem of multi-domain sampling of zoned zircons. Epsilon values are adjusted for the age (t) of a zircon grain (Item 7, see footnote 1). Notably,

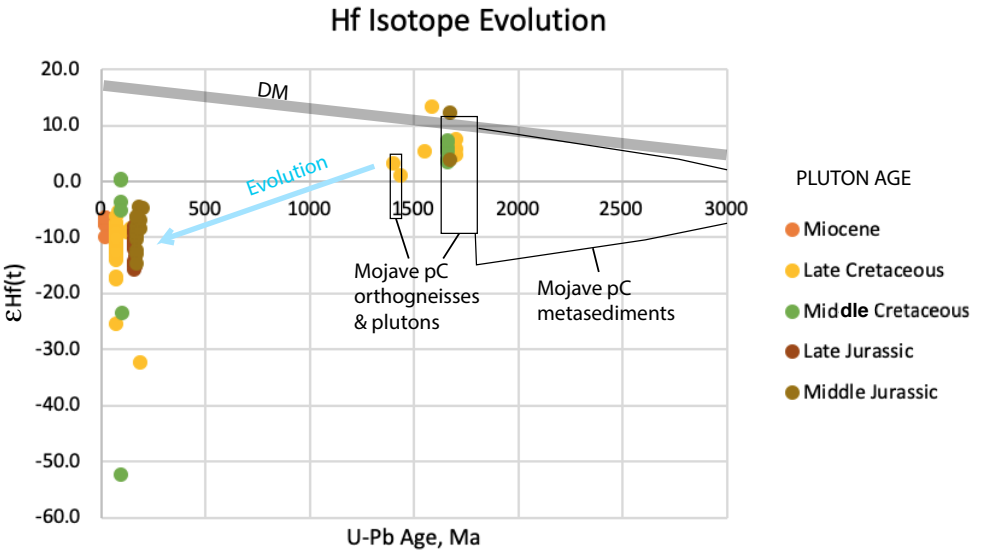

Figure 5. Zircon-grain $\varepsilon Hf_{(t)}$ plotted against $^{206}Pb/^{238}U$ concordant ages. The analytical precision is equivalent to ~1.5 epsilon units (at 2σ). Blue arrow shows direction of model $\varepsilon Hf_{(t)}$ evolution assuming crustal average $^{176}Lu/^{177}Hf = 0.015$. Boxes show fields of Precambrian (pC) rocks from the Mojave (Wooden et al., 2013; Holland et al., 2018). DM—depleted-mantle evolution model.

Mesozoic and Cenozoic grains nearly all have negative epsilon Hf values. Mesozoic and Cenozoic arrays of age-corrected epsilon values range from about –5 to –15, excluding outliers. Data for Proterozoic xenocrystic zircon (dated ca.1.8–1.3 Ga) generally plot in or above the upper part of fields (boxes in Fig. 5) that show reported $\varepsilon Hf_{(t)}$ ranges of exposed Proterozoic orthogneisses and granitoids in the Mojave province (Wooden et al., 2013). Zircons in a ca. 1660 Ma granite gneiss that we analyzed also range in $\varepsilon Hf_{(t)}$ in and above those boxes (not shown; see Items 6 and 7).

The blue arrow shows the direction of isotopic evolution modeled for the commonly assumed average crustal value of $^{177}Lu/^{176}Hf$ = 0.015 (e.g., Shaw et al., 2011). The modeling otherwise follows Wooden et al. (2013) in Lu-Hf parameters and assumption of a depleted mantle model (DM). See Item 3 of the Supplemental Material (footnote 1).

No correlation to rock composition is apparent for any of the magmatic episodes, as zircon in Cretaceous and Jurassic quartz diorites is not noticeably different in Hf isotopes from zircon in more silicic rocks in the same rock age groups. Calculated Hf model ages lie mostly between 2200 and 1400 Ma, averaging 1700 ± 190 Ma for zircon in the two Middle Jurassic rocks, 1820 ± 160 Ma in the three Late Jurassic rocks, a wide 4200–1060 Ma range in middle Cretaceous granodiorite (1920 ± 830 Ma), 1780 ± 350 Ma in the seven Late Cretaceous rocks, and 1500 ± 80 Ma in the Miocene diorite. Paleoproterozoic xenocrystic zircon $\varepsilon Hf_{(t)}$ values lie in and above the upper part of the fields reported from Paleoproterozoic basement rocks (Fig. 5).

Figures 6 and 7 explore temporal patterns in the Hf data, including previously published zircon Hf isotopic data for six other Cretaceous and Miocene rocks in the study area (Fisher et al., 2017; Chapman et al., 2018). Figure 6 displays all measured $^{176}Hf/^{177}Hf$ ratios (not age-corrected) including for undated or poorly dated zircons, grouped by pluton age group. Most of the data populate two bands highlighted across Figure 6, suggesting shared magmatic sources. The lower band includes Proterozoic xenocrysts and corresponds to many observed ratios in zircons from Proterozoic orthogneisses in the Mojave province (bar at far right of the diagram; Wooden et al., 2013). The band equates to Proterozoic material having model ages ca. 1730 Ma assuming $^{176}Lu/^{177}Hf$ = 0.015. It also includes some grains dated as Mesozoic.

The upper band surrounds overlapping Hf isotope signatures of the magmatic Jurassic and Late Cretaceous zircons. It corresponds to model ages of 2040–1600 Ma for an assumed crystallization age of 75 Ma and $^{176}Lu/^{177}Hf$ = 0.015. Some Hf isotope ratios from Miocene and middle Cretaceous rocks extend above the upper band (>0.2825). Isolated points also fall in between the bands, nearly all relating to discordant U-Pb ages (multiple grain domains sampled). Data points well below the lower band (<0.2828) correspond to model ages 4–2 Ga.

The data show consistent differences between age groups (Fig. 6). Cretaceous samples are the most variable in $^{176}Hf/^{177}Hf$, reflecting their large degree of inherited zircon. Our data from the

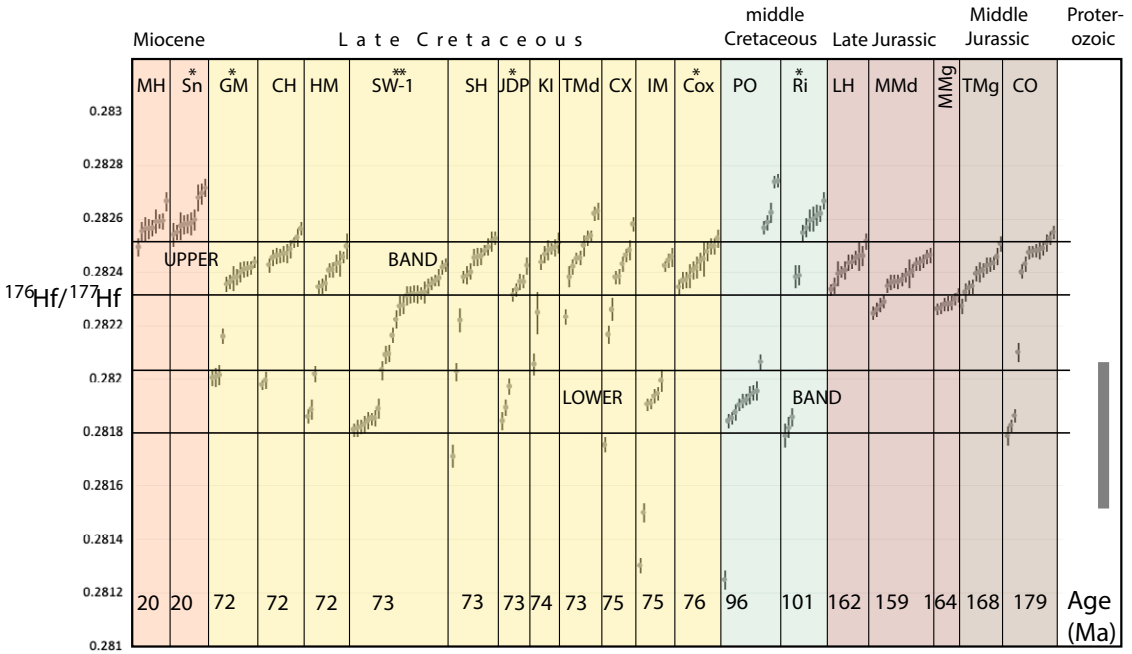

Figure 6. Individually plotted modern $^{176}Hf/^{177}Hf$ ratios (t = 0) for all measured zircons from our 14 samples, plus samples from six other Phanerozoic plutons (asterisks) reported from within the study area and located in Figure 2 (*Chapman et al., 2018; **Fisher et al., 2017; Items 1 and 7, see text footnote 1). Colors designate the pluton age groups. Approximate magmatic ages are shown at the bottom. The upper highlighted horizontal band (see text) includes Mesozoic magmatic grains (modern epsilon values at t = 0 would range –10 to –17, lower than for the age of the zircons). The lower band (epsilons –26 to –35 at t = 0) includes dated inherited Proterozoic zircons. The bar at the right ("Proterozoic") represents range of values for 1780–1630 Ma Proterozoic granitoids and orthogneisses from the Mojave province ($\varepsilon Hf_{(t)}$ +11 to –10; Wooden et al., 2013).

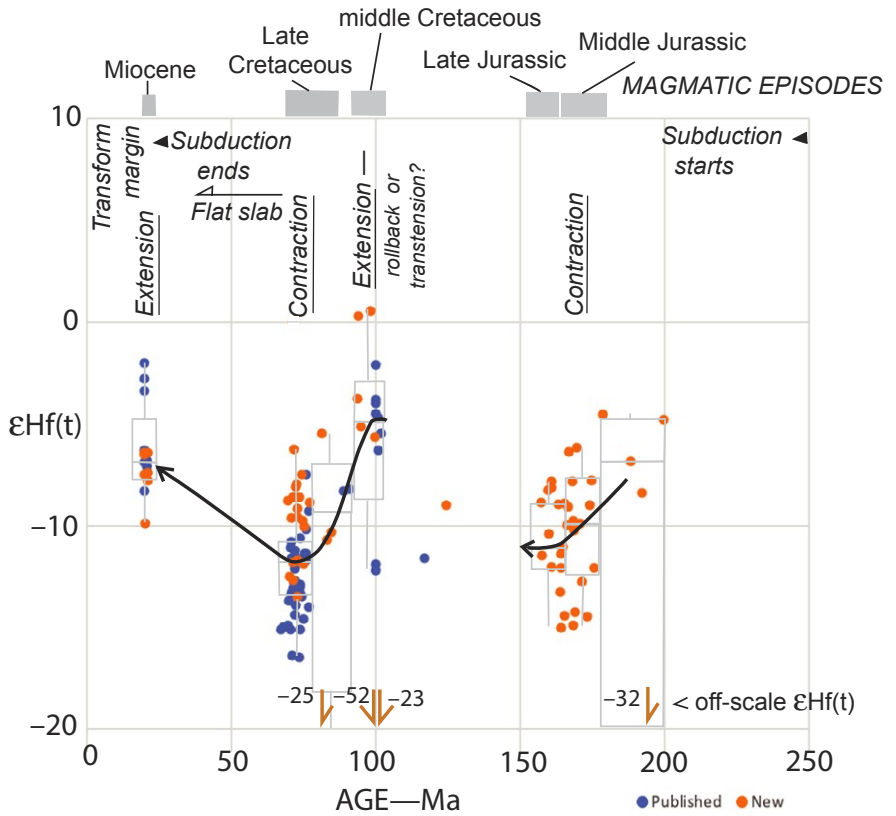

Figure 7. Magmatic episodes and Hf epsilon values for concordant and near-concordant dated Mesozoic and Cenozoic zircons in the study area (including data from Fisher et al., 2017, and Chapman et al., 2018). Black paths of interpreted temporal changes in εHf are guided by median values in (gray) box-and-whisker bins. Colored arrows point toward four off-scale epsilon values. Isotopic pull-downs during the higher-flux episodes are here interpreted to signal convergent contraction; whereas, pull-ups are interpreted to signal extension and crustal thinning. Subduction from 250 to 20 Ma at this part of the North American margin included switches between dextral and sinistral obliquities and rapid switching between contraction and extension (e.g., Walker et al., 2002).

Late Cretaceous rocks closely resemble $^{176}Hf/^{177}Hf$ patterns in the four other previously reported ca. 76–72 Ma plutons in the study area (Fisher et al., 2017; Chapman et al., 2018). Middle Cretaceous granodiorite (sample PO, Fig. 2) uniquely contains both the highest and lowest ratios but otherwise resembles Hf isotopic values previously reported from a ca. 101 Ma quartz monzodiorite from the Turtle assemblage (Ri, Figs. 2 and 6). Miocene diorite (MH) compares well in its zircon Hf isotopes to a previously reported ca. 20 Ma dacitic rock (Sn). Jurassic samples have few values in the lower band, reflecting a lack of inherited Proterozoic zircons except in Middle Jurassic sample CO, which resembles Late Cretaceous rocks in its Hf isotopic compositions and its abundant inherited zircon. Hf ratios from two Late Jurassic plutons 7 km apart (MMd and MMg; Fig. 2) plot slightly below the upper band, corresponding to $\varepsilon Hf_{(t)}$ values –12 to –15 and model ages ca. 2 Ga.

Figure 7 displays secular differences in $\varepsilon Hf_{(t)}$ values for concordantly and near-concordantly dated Mesozoic and Cenozoic zircons including previously published data. Magmatic grains in the Late Cretaceous and Jurassic rocks share similar ranges in $\varepsilon Hf_{(t)}$, in contrast to Miocene and middle Cretaceous rocks. Mean $\varepsilon Hf_{(t)}$ values for magmatic grains (dating within 10% of the pluton age) are –6.5 in the two Miocene rocks (lower values occur in plutons just north of the study area; McDowell et al., 2016), –6 and –8.5 in the two middle Cretaceous rocks (but diverse in PO), and –9 to –11 in most Late Cretaceous and Jurassic rocks except a mean of –14 in a highly peraluminous Late Cretaceous granite reported by Fisher et al. (2017). Some middle Cretaceous zircons (in PO) are the least negative in $\varepsilon Hf_{(t)}$ value (three grains +0.3 to –5; Fig. 5). Four $\varepsilon Hf_{(t)}$ values from Cretaceous intrusions (including for one crystal dated as Jurassic) are more negative, from –23 to –52.

INTERPRETATION OF Hf ISOTOPIC COMPOSITIONS

The range in Hf isotopic composition for each sample exceeds the associated analytical uncertainty (~1.5 epsilon units; see Item 2, footnote 1), indicating that each pluton is a hybrid of multiple sources. The clustered ranges of $\varepsilon Hf_{(t)}$ for most magmatic Late Cretaceous and Jurassic zircons project back along model evolution paths (arrow, Fig. 5) toward the Proterozoic xenocryst $\varepsilon Hf_{(t)}$ values, as if the inherited zircon was contributed from the same range of materials from which the Mesozoic magmas were sourced. The xenocryst values lay toward the upper end of values (boxes) shown for Proterozoic plutonic and metaplutonic rocks (Fig. 5; Wooden et al., 2013; Holland et al., 2018). This indicates to us that the Jurassic and Late Cretaceous magmas were sourced from material slightly more primitive in $^{176}Hf/^{177}Hf$ than most of the exposed Paleoproterozoic plutonic rocks, but comparable to some isotopically primitive ca. 1.73 Ga plutons (Holland et al., 2018) and some measured Paleoproterozoic diorite, trondhjemite (Wooden et al., 2013), and even granite (Kilbeck Gneiss; Supplemental

Material, see footnote 1). Deep Mojave province lower-crust materials could be appropriate melt sources to explain the isotopic signal. Small contributions from mantle end-member sources (high Lu/Hf) might also have played a role. Mesozoic crustal thickening is believed to have depressed the lower crust to deep levels by Late Cretaceous time (Miller et al., 1992; Hanchar et al., 1994; Chapman et al., 2015; Economos et al., 2021). Likely sources include intermediate to mafic Paleoproterozoic granitoids, residue from earlier crustal melting, and/or basaltic underplate (Miller et al., 1990; Miller and Wooden, 1994; Economos et al., 2010a).

The upper bands of Hf isotopic ratios in Figure 6 are consistent with rocks produced mainly or entirely by anatexis of Proterozoic material of the Mojave crustal province. The lower band corresponds to Proterozoic xenocrysts. We interpret the rare low $^{176}Hf/^{177}Hf$ values below the lower band in some Cretaceous plutons (Fig. 6), some dating as Mesozoic, as contributions from early Paleoproterozoic to Archean material, such as detrital components in exposed supracrustal gneisses characterized as Vishnu basin in Mojave crust (Holland et al., 2018). Such an origin is consistent with xenoliths of restite carried from the deep crust in Miocene dikes (Miller et al., 1992; Hanchar et al., 1994). Miller et al. (1992) interpreted the xenoliths, together with xenocrystic zircon and other accessory minerals in the Old Woman–Piute batholith, as residue from partial melting at depths of ~40 km of garnet-bearing, lower-crustal metasedimentary and meta-igneous sources that produced the Late Cretaceous granitoids (Miller et al., 1992; see also Fisher et al., 2017). Judging from our finding of sparse Jurassic zircon xenocrysts, the Late Cretaceous deep crustal melt-accumulation regions likely also included remnants from the Jurassic magmatism.

Hf isotope ratios above the upper band (Fig. 6) and some high $\varepsilon Hf_{(t)}$ values (Figs. 5 and 7) in middle Cretaceous rocks (+0.5 to –6) and Miocene rocks (–2 to –10) imply more juvenile contributions. No effects are apparent in our data of any suggested asthenosphere-derived magma in the Late Cretaceous (Leventhal et al., 1995) or the early Miocene (Howard, 1993).

Differences in zircon Hf isotopic character and presence of xenocrysts among the five magmatic episodes (Fig. 6) imply differences in melt generation sources.

Middle Jurassic

Magmatic zircon $\varepsilon Hf_{(t)}$ ranging between –4 and –15 in the Middle Jurassic plutons is consistent with origins dominated by crustal materials. Middle Jurassic granodiorite CO has a high Sr/Y of 37 compatible with a deep origin in thick crust (cf. Chapman et al., 2015), in keeping with its uniquely abundant inherited zircon among the sampled Jurassic rocks. Similar characteristics intriguingly were mimicked later in the Late Cretaceous magmatic episode (Howard et al., 2016).

Late Jurassic

Moderate ranges of $\varepsilon Hf_{(t)}$ of about –15.5 to –6 in the three sampled plutons of the Bristol Mountains sequence accompany and help track the Jurassic arc transition at ca. 164 Ma to light rare-earth element (LREE)–enriched, alkali-calcic early Late Jurassic magmas (Barth et al., 2017). The scarcity of xenocrysts in our samples is consistent with the idea that they represent hot (>800 °C), dry alkali-calcic magmas, undersaturated in zircon, accumulated by extensive melting of restricted parts of the crustal column and triggered by melts rising from mantle lithosphere (Fox and Miller, 1990; Barth et al., 2017). Model Hf ages ca. 2000 Ma (and $^{176}Lu/^{177}Hf$ = 0.282260–0.282282) for zircons both in a quartz diorite and a nearby granite (MMd and MMg, Fig. 2) point toward a localized crustal source.

Middle Cretaceous

High $\varepsilon Hf_{(t)}$ values (to barely positive values) for some magmatic zircon in middle Cretaceous plutons are consistent with the more primitive Rb/Sr and Sm/Nd isotopic nature of middle Cretaceous rocks compared to other Mesozoic plutons in this region (Allen et al., 1995; Rämö et al., 2002). High middle Cretaceous values of $^{176}Hf/^{177}Hf$, and $\varepsilon Hf_{(t)}$, higher than for Miocene (see Miocene section below), likely signal small contributions from asthenosphere. On the other hand, middle Cretaceous magma also carried Precambrian crust contributions, namely zircon $\varepsilon Hf_{(t)}$ values as low as –52 and Proterozoic xenocrysts making up more than half of sample PO's dated zircon. The middle Cretaceous episode's Hf isotopic character is consistent with small contributions from convecting asthenospheric mantle mixed into dominant partial melts of Mojave crust.

Late Cretaceous

Low values of $^{176}Hf/^{177}Hf$ and $\varepsilon Hf_{(t)}$ and abundant Proterozoic xenocrysts in the ca. 75 Ma Late Cretaceous rocks support previous inferences that the Late Cretaceous plutons originated mainly from partial melting of deep materials such as Precambrian Mojave crust. Tight $\varepsilon Hf_{(t)}$ arrays of most well-dated Late Cretaceous zircons (mean, –10.3) are consistent with evolution mainly from sources similar in age to exposed Paleoproterozoic plutonic rocks (Fig. 5). Rarer much lower values ($\varepsilon Hf_{(t)}$ to –32; $^{176}Hf/^{177}Hf$ as low as 0.2812) implicate contributions from source materials more ancient than 1800 Ma such as Vishnu basin material. Late Cretaceous magmatism presumably preceded a subducting flat slab (cf. Economos et al., 2021). Low whole-rock Y and high Sr/Y and moderately low initial Sr ratios implicate derivation from garnet-bearing sources in deep lower crust (Miller et al., 1992; Economos et al., 2010b, 2021) or delaminated former crust (Hildebrand and Whalen, 2017) or arclogite (Chapman et al., 2020).

Miocene

Early Miocene diorite sample MH's moderately high MgO, Cr, and Ni implicate mantle material as a major source of its melt. The diorite's range of $\varepsilon Hf_{(t)}$ (–1 to –10) resembles McDowell et al.'s (2016) estimate of –2 to –8 for Mojave mantle lithosphere

in the Miocene based on the Nd isotopic character of volcanic rocks. A range of εHf values essentially identical to that of MH was reported for an early Miocene dacitic rock (Sn in fig. 6, from Chapman et al., 2018), which we interpret to indicate that similar mantle sources led to a range of magma compositions. Multiple isotopic systems in similar Mojave synextensional Miocene rocks north of the study area are also consistent with mantle-lithosphere sources, but mixed varyingly with crustal components, as expressed in whole rock Nd and Sr isotope values and in an εHf(t) range from –5 to –20 (Miller et al., 2009; Ryan, 2011; Ryan, 2011; McDowell et al., 2016).

EVOLVING MAGMATISM AND TECTONISM

Continental magmatic arcs typically are associated with magmas triggered by fluids rising from a subducting slab that drive partial mantle melts to rise into and interact with crust. The changing Hf signals in our study over a 150 m.y. period imply shifting magmatic source contributions. Arrow paths in Figure 7 portray sequences of variation in Hf isotopic composition of magmatic zircon. The secular differences accompany cyclic changes in magmatic flux in which magmatic lulls in this part of the Mojave Desert at 160–100 Ma, 95–80 Ma, and 70–25 Ma separate the magmatic episodes. Isotopic pull-ups accompany the lower-flux middle Cretaceous and early Miocene episodes following pull-downs in the higher-flux Jurassic and Late Cretaceous episodes. The isotopic pull-downs and pull-ups in this geographically restricted sample of the Cordillera deny an explanation (Chapman and Ducea, 2019) that relates secular isotopic changes to arcs migrating in distance from the continental edge.

The lowering isotopic shift from Middle Jurassic high-K calc-alkalic to Late Jurassic alkali-calcic arc magmatism indicates increasing influence of crustal or more Hf isotopically mature crustal sources. The smaller middle Cretaceous pulse of calcic plutons followed a ca. 60 Ma magmatic lull. The plutons of this later pulse contain inheritance strongly signaling crustal contributions, but also show the least matured magmatic-zircon Hf isotopes in our data set, implying a more juvenile contribution.

The younger shift back after a 20 m.y. lull to the big Late Cretaceous flare-up produced lower magmatic εHf values indicative of wholly dominant crust-like sources. This isotopic pull-down coincided regionally with eastward-migrating plutonism associated with s eastward-migrating flat-slab subduction of an oceanic plateau in the Fallon plate, and associated Laramide tectonism (Coney and Reynolds, 1977; Henderson et al., 1984; Saleeby, 2003; Wells and Hoisch, 2008; Liu et al., 2010; Heller and Liu, 2016; Chapman et al., 2018). Possible triggers driving the Late Cretaceous magmatism include an arc progressing eastward in front of shallow-angle subduction, underflow of fertile lithosphere, or upwelling due to mantle delamination or to westward extrusion toward a collapsing arc (Wells and Hoisch, 2008; DeCelles et al., 2009; Chapman et al., 2010, 2020; Hildebrand and Whalen, 2017; Economos et al., 2021). Then, after a 55 Ma magmatic lull, the lower-flux early Miocene magmatism, during post-subduction extensional thinning of the crust, produced plutons with a pull-up in zircon εHf to values consistent with hybrid sources including major contributions from enriched old mantle lithosphere.

One hypothesis explains isotopic pull-downs in arcs as recording subduction-driven contraction, whereas pull-ups represent thinned crust and greater mantle contributions during rollback of the subducting slab (Kemp et al., 2009; Nelson and Cottle, 2018; Poole et al., 2020). Some models relate high-flux arc-type magmatism to slab breakoff (Wells and Hoisch, 2008; Hildebrand and Whalen, 2017).

A different model correlates pull-downs to cyclic high-flux magmatism and elaborates that the high-flux events result from convergent thickening and introduction of fertile lithosphere for melting by underflow from farther inboard in the retroarc; subsequent isotopic pull-ups result when the magmatism's dense crustal residue founders into the mantle, thins the crust, and slows the crustal melting (DeCelles et al., 2009). The imaging of Mojave-like deep crust by our Mesozoic plutons suggests a possible constraint on that model. The Yavapai and other crustal provinces east of the eastern Mojave study area (Fig. 1) lack components more ancient than ca. 1800 Ma that could explain our deeply negative εHf values. Sparse Mesozoic zircon $\varepsilon Hf_{(t}$ more negative than –20 (Fig. 7) and $^{176}Hf/^{177}Hf$ below the lower band (Fig. 6), together with Pb isotope evidence (Wooden et al., 1988), are consistent with local Mojave province sources for the Mesozoic plutons rather than any more eastern sources introduced by the westward underflow predicted in the DeCelles et al. (2009) model. Younger flat-slab subduction in the Paleogene, however, may have underthrust material *eastward* (Luffi et al., 2009; Chapman et al., 2020).

The middle Cretaceous Hf pull-up and its coincidence with development of a deep McCoy Mountains Formation basin (Barth et al., 2004) potentially could represent two signals of backarc extension from transtension or from rollback of a subducting slab. They additionally could relate the moderate middle Cretaceous magmatic flux to a lower ratio of available fertile continental sources relative to sub-continental magma compared to younger and older higher-flux episodes. Allen et al. (1995) suggested that middle Cretaceous magmatism in our study area interacted less with the crust than did the more voluminous Late Cretaceous event. The middle Cretaceous $\varepsilon Hf_{(t)}$ values and low middle Cretaceous Sr_i values (Table 1) resemble the character of the contemporaneous larger, more outboard main Sierra Nevada middle Cretaceous arc. Hf model ages for magmatic zircons in PO are >1050 Ma, just a little higher than those for middle Cretaceous batholiths in the Sierra Nevada (1300–750 Ma) and the Peninsular Ranges (900–200 Ma with rare model ages 2300–1700 Ma) (Fig. 1; Shaw et al., 2014). The model ages for those main-arc batholiths, which lie west of exposed Precambrian basement, imply some involvement of ancient crust and/or lithosphere, although not as markedly as in our backarc PO granodiorite. Modern backarc magmatic belts typically form above slab depths of ~170 km, deeper than for main arcs (Tatsumi, 2005), but typically are alkalic rather than calcic like the middle Cretaceous rocks of the eastern Mojave study area. On the premise that the middle Cretaceous isotopic pull-up signals extension, its age coincidence with more outboard high-flux Sierra Nevada, Salinia, and Peninsular Ranges batholith events may contradict a prediction

that those high-flux events necessarily represent strong convergence (DeCelles et al., 2009).

The much later early Miocene lower-flux magmatism and isotopic pull-up is in an ambiguous tectonic setting, as its timing and geography coincides with part of a westward late Paleogene sweep of Cordilleran arc magmatism that has been related to slab steepening and rollback (Chapman et al., 2020; Timmermans et al., 2020), but also approximately coincides with the inception of a slab window at this latitude as convergence transitioned to margin-parallel transform tectonics (Engebretson et al., 1984; Atwater and Stock, 1998). Tectonic extension that accompanied the early Miocene magmatism could relate to thinned lithosphere above a slab window, to slab rollback, and/or to breaking of a narrow lithosphere bridge (Armstrong and Ward, 1991) between the warmed and extending Mexico and Nevada parts of the Basin and Range province. The more juvenile Miocene isotopic character importantly signals that the Laramide magmatic style had ended.

Time-varying patterns of Hf and Nd isotopic character in subduction-related magmatic rocks are seen also from elsewhere in western North America (Mendoza and Suastegui, 2000; Piercey et al., 2003; Gaschnig et al., 2011; Girardi et al., 2012; Klemetti et al., 2014; Chapman et al. 2018; Cecil et al., 2019) as well as western South America (Haschke et al., 2002; Mamani et al., 2010; Jones et al., 2015; Pepper et al., 2016; Poole et al., 2020), West Antarctica (Nelson and Cottle, 2018), and eastern Australia (Kemp et al., 2009; Siégel et al., 2020). The Mojave results verify the typical cyclical changes in isotopic character as correlated with magmatic flux, with isotopic pull-downs indicative of more crustal involvement occurring during higher-flux episodes (DeCelles et al., 2009). Two lower-flux isotopic pull-ups imply more mantle involvement in magmatism, likely associated with tectonic plate interactions that included extension.

CONCLUSIONS

The combined zircon Lu-Hf isotopic and xenocryst data allow insights into melt sources and their relation to evolving tectonics of a sample of the North American Cordillera in the southwest United States. Varied mixtures of three types of end-member magmatic sources can account for the Hf isotopic results and xenocrystic zircon cores: (1) signals of Precambrian Mojave province crust sources dominating all the Mesozoic rocks, (2) juvenile material such as asthenosphere as a small component in middle Cretaceous rocks, and (3) enriched ancient mantle lithosphere of the Mojave province as a notable source component for early Miocene rocks. The Mesozoic plutons' Hf isotopes are consistent with derivation largely from deep Mojave crust including dominant 1800–1600 Ma material, some ca. 1400 Ma material (from xenocrystic evidence), and some ancient detrital material of early Paleoproterozoic to Archean parentage. We infer that subduction-related Mesozoic fluids and magmas variably interacted with a variety of lower crust materials to produce anatectic-rich magmas that eventually coalesced into the middle and upper-crustal plutons now exposed.

The succession of arc magmatic events in Proterozoic crust in this area show cyclical changes in isotopic signals that correlate to magmatic flux. Episodic plutonism into Mojave crust U-Pb-dated at ca. 170, 160, 100, 75, and 20 Ma confirms the common presence of inherited old zircon in Cretaceous plutons and some late Middle Jurassic plutonic rock. Zircon Lu-Hf isotopic data show that Mesozoic magmas included major components of partial melts derived from material similar in age to exposed Proterozoic plutons and orthogneisses in the Mojave province but slightly less mature in Hf isotopes, perhaps on average less felsic. A small minority of zircons having very low values of Hf isotope ratios in some middle Cretaceous and Late Cretaceous rocks are interpreted to be derived from pre-1800 Ma detrital components in Paleoproterozoic supracrustal gneisses of the Mojave crustal province.

Middle Cretaceous plutons additionally show a conspicuous isotopic pull-up to less mature Hf isotopes, which may record a small asthenosphere component of magma in addition to dominant incorporated crustal material. A second isotopic Hf isotopic pull-up during early Miocene magmatism and extension is attributed to magma contributions from enriched old mantle lithosphere. The sequential Mesozoic subduction-related magmas as well as the Miocene episode variably interacted with the Precambrian lower crust.

As in other magmatic arcs (DeCelles et al., 2009), higher-flux magmatic pulses (here in the Jurassic and Late Cretaceous) record isotopic pull-downs in epsilon Hf values and pull-ups during lower-flux (middle Cretaceous and Miocene) pulses. The pull-downs and pull-ups correlate with magmatic flux and not straightforwardly with distance from the plate edge. Crustal contributions conspicuously dominated the higher-flux magmatic episodes and contributed to the two lower-flux episodes.

We interpret the higher-flux Jurassic and Late Cretaceous events to record convergent subduction tectonics, whereas we suggest the lower-flux, slightly more isotopically juvenile middle Cretaceous and Miocene pulses reflect extension, as in transtension, slab-rollback, or slab-window tectonic environments. The middle Cretaceous episode occurred in a backarc position relative to a contemporaneous high-flux arc that produced the Sierra Nevada, Salinia, and Peninsular Ranges batholiths closer to the plate margin. Middle Cretaceous backarc plutons ca. 100–90 Ma in the Mojave resemble the Sierra-to-Peninsular Ranges arc compositionally and isotopically. If crustal thinning played a role in this middle Cretaceous Mojave hinterland episode, it may lend support to an extensional tectonic environment for the contemporaneous Sierra Nevada and Peninsular Ranges batholiths (Ward, 1991) rather than a contractional environment (DeCelles et al., 2009).

ACKNOWLEDGMENTS

We honor Calvin Miller's research leadership in igneous processes and our long friendship with him. Stirling Shaw (1933–2013), an exceptional man, warm friend, and long-time collaborator on Mojave plutonism performed the geochemical and isotopic analyses and initial discussions for preparation of this paper. We are grateful to Jamey Jones, Rita Economos, Calvin Miller, Jonathan Miller, and an anonymous reviewer for insightful review suggestions to improve the manuscript. Jonathan Miller and Robert Powell suggested editorial improvements. We thank Joe Wooden, Barbara John, Dave Miller, Andy Barth, Lawford Anderson, Rita Economos, and Jim Wright for helpful discussions. Barbara John mapped some of the plutons and

provided the Late Cretaceous sample CH. Bruce Bryant led us to the middle Cretaceous pluton (sample PO). Norman Pearson provided guidance for the laboratory isotopic analyses.

REFERENCES CITED

Allen, C.M., Wooden, J.L., Howard, K.A., Foster, D.A., and Tosdal, R.M., 1995, Sources of the Early Cretaceous plutons in the Turtle and West Riverside Mountains, California: Anomalous Cordilleran Interior plutons: Journal of Petrology, v. 36, p. 1675–1700.

Anderson, J.L., and Bender, E.E., 1989, Nature and origin of Proterozoic A-type granitic magmatism in the southwestern United States of America: Lithos, v. 23, p. 19–52, https://doi.org/10.1016/0024-4937(89)90021-2.

Anderson, J.L., and Cullers, R.L., 1990, Middle to upper crustal plutonic construction of a magmatic arc: An example from the Whipple Mountains metamorphic core complex, *in* Anderson, J.L., ed., The Nature and Origin of Cordilleran Magmatism: Geological Society of America Memoir 174, p. 47–70, https://doi.org/10.1130/MEM174-p47.

Anderson, J.L., Barth, A.P., Young, E.D., Bender, E.E., Davis, M.J., Faber, D.L., Hayes, E.M., and Johnson, K.A., 1992, Plutonism across the Tujunga–North American terrane boundary; a middle to upper crustal view of two juxtaposed magmatic arcs, *in* Bartholomew, M.J., Hyndman, D.W., Mogk, D.V., and Mason, R., eds., Characterization and Composition of Ancient (Precambrian to Mesozoic) Continental Margins: Proceedings of the Eighth International Conference on Basement Tectonics, August 1988, Butte, Montana: Dordrecht, Boston, London, Kluwer Academic Publishers, p. 205–230.

Armstrong, R.L., and Ward, P.L., 1991, Evolving geographic patterns of Cenozoic magmatism in the North American Cordillera: The temporal and spatial association of magmatism and metamorphic core complexes: Journal of Geophysical Research, v. 96, p. 13,201–13,224, https://doi.org/10.1029/91JB00412.

Atwater, T., and Stock, J., 1998, Pacific–North America plate tectonics of the Neogene southwestern United States: An update: International Geology Review, v. 40, p. 375–402, https://doi.org/10.1080/00206819809465216.

Barth, A.P., and Wooden, J.L., 2010, Coupled elemental and isotopic analyses of polygenetic zircons rom granitic rocks by ion microprobe, with implications for melt evolution and the sources of granitic magmas: Chemical Geology, v. 277, p. 149–159, https://doi.org/10.1016/j.chemgeo.2010.07.017.

Barth, A.P., Tosdal, R.M., Wooden, J.L., and Howard, K.A., 1997, Triassic plutonism in southern California, Southward younging of arc initiation along a truncated continental margin: Tectonics, v. 16, p. 290–304, https://doi.org/10.1029/96TC03596.

Barth, A.P., Wooden, J.L., Jacobsen, C.E., and Probst, K., 2004, U-Pb geochronology and geochemistry of the McCoy Mountains Formation, southeastern California: A Cretaceous retroarc foreland basin: Geological Society of America Bulletin, v. 116, p. 142–163, https://doi.org/10.1130/B25288.1.

Barth, A.P., Wooden, J.L., Coleman, D.S., and Vogel, M.B., 2009, Assembling and disassembling California: A zircon and monazite geochronologic framework for Proterozoic crustal evolution in southern California: The Journal of Geology, v. 117, p. 221–239, https://doi.org/10.1086/597515.

Barth, A.P., Wooden, J.W., Miller, D.M., Howard, K.A., Fox, L.K., Schermer, E.R., and Jacobson, C.E., 2017, Regional and temporal variability of melts during a Cordilleran magma pulse: Age and chemical evolution of the Jurassic arc, eastern Mojave Desert, California: Geological Society of America Bulletin, v. 129, p. 429–448, https://doi.org/10.1130/B31550.1.

Beard, B.L., and Johnson, C.M., 1997, Hafnium isotope evidence for the origin of Cenozoic basaltic lavas from the southwestern United States: Journal of Geophysical Research. Solid Earth, v. 102, p. 20,149–20,178, https://doi.org/10.1029/97JB01731.

Bender, E.E., Morrison, J., Anderson, J.L., and Wooden, J.L., 1993, Early Proterozoic ties between two suspect terranes and the Mojave crustal block of the southwestern U.S.: The Journal of Geology, v. 101, p. 715–728 https://doi.org/10.1086/648270.

Bennett, S.E.K., Darin, M.H., Dorsey, R.J., Skinner, L.A., Umhoefer, P.J., and Oskin, M.E., 2016, Animated tectonic reconstruction of the lower Colorado River region: Implications for late Miocene to present deformation, *in* Reynolds, R.E., ed., Going LOCO, Investigations along the lower Colorado River: Northridge, California State University Desert Studies Center, 2016 Desert Symposium Field Guide and Proceedings, April 2016: Northridge, California State University, 2016 Desert Symposium, p. 73–86.

Bennett, V.C., and DePaolo, D.J., 1987, Proterozoic crustal history of the western United States as determined by neodymium isotopic mapping: Geological Society of America Bulletin, v. 99, p. 674–685, https://doi.org/10.1130/0016-7606(1987)99<674:PCHOTW>2.0.CO;2.

Bradshaw, T.K., Hawksworth, C.J., and Gallagher, T., 1993, Basaltic volcanism in the southern Basin and Range: No role for a mantle plume: Earth and Planetary Science Letters, v. 116, p. 45–62, https://doi.org/10.1016/0012-821X(93)90044-A.

Bryant, B., and Wooden, J.L., 2008, Geology of the northern part of the Harcuvar Complex, west-central Arizona: U.S. Geological Survey Professional Paper 1752, 52 p.

Bryant, B., Wooden, J.L., and Nealy, L.D., 2001, Geology, geochronology, geochemistry, and Pb-isotopic compositions of Proterozoic rocks in the Poachie region, west-central Arizona—A study of the east boundary of the Proterozoic Mojave crustal province: U.S. Geological Survey Professional Paper 1639, 54 p., https://doi.org/10.3133/pp1639.

Burchfiel, B.C., and Davis, G.A., 1975, Nature and controls of Cordilleran orogenesis, western United States: Extensions of an earlier synthesis: American Journal of Science, v. 275A, p. 363–396.

Burchfiel, B.C., and Davis, G.A., 1981, Mojave Desert and environs, *in* Ernst, W.G., ed., The Geotectonic Development of California, Rubey Volume I: Englewood Cliffs, New Jersey, Prentice-Hall, p. 217–252.

Calzia, J.P., DeWitt, E., and Nakata, J.K., 1986, U-Th-Pb age and initial strontium isotopic ratios of the Coxcomb Granodiorite, and a K-Ar date of olivine basalt from the Coxcomb Mountains, southern California: Isochron-West, v. 47, p. 3–7.

Campbell-Stone, E., John, B.E., Foster, D.A., Geissman, J.W., and Livaccari, R.F., 2000, Mechanisms for accommodation of Miocene extension: Low-angle normal faulting, magmatism, and secondary breakaway faulting in the southern Sacramento Mountains, southeastern California: Tectonics, v. 19, p. 566–587 https://doi.org/10.1029/1999TC001133.

Cecil, M.R., Ferrer, M.A., Riggs, N.R., Marsaglia, K., Kylander-Clark, A., Ducea, M.N., and Stone, P., 2019, Early arc development recorded in Permian–Triassic plutons of the northern Mojave Desert region, California, USA: Geological Society of America Bulletin, v. 131, p. 749–765, https://doi.org/10.1130/B31963.1.

Chapman, A.D., Kidder, S., Saleeby, J.B., and Ducea, M.N., 2010, Role of extrusion of the Rand and Sierra de Salinas schists in Late Cretaceous extension and rotation of the southern Sierra Nevada and vicinity: Tectonics, v. 29, https://doi.org/10.1029/2009TC002597.

Chapman, A.D., Rautela, O., Shields, J., Ducea, M.N., and Saleeby, J., 2020, Fate of the lower lithosphere during shallow-angle subduction: The Laramide example: GSA Today, no. 1, v. 30, https://doi.org/10.1130/GSATG412A.1.

Chapman, J.B., and Ducea, M.N., 2019, The role of arc magmatism in Cordilleran orogenic cyclicity: Geology, v. 47, p. 627–631, https://doi.org/10.1130/G46117.1.

Chapman, J.B., Ducea, M.N., DeCelles, P.G., and Profeta, L., 2015, Tracking changes in crustal thickness during orogenic evolution with Sr/Y: An example from the North American Cordillera: Geology, v. 43, p. 919–922, https://doi.org/10.1130/G36996.1.

Chapman, J.B., Dafov, M.N., Gehrels, G., Ducea, M.N., Valley, J.W., and Ishida, A., 2018, Lithospheric architecture and tectonic evolution of the southwestern U.S. Cordillera: Constraints from zircon Hf and O isotopic data: Geological Society of America Bulletin, v. 130, p. 2031–2046, https://doi.org/10.1130/B31937.1.

Coney, P.J., and Reynolds, S.J., 1977, Cordilleran Benioff zones: Nature, v. 270, p. 403–406, https://doi.org/10.1038/270403a0.

Daley, E.E., and DePaolo, D.J., 1992, Isotopic evidence for lithospheric thinning during extension: Southeastern Great Basin: Geology, v. 20, p. 104–108, https://doi.org/10.1130/0091-7613(1992)020<0104:IEFLTD>2.3.CO;2.

Davis, M.J., Farber, D.L., Wooden, J.L., and Anderson, J.L., 1994, Conflicting tectonics?—Contraction and extension at middle and upper crustal levels along the Cordilleran Late Jurassic arc, southeastern California: Geology, v. 22, p. 247–250, https://doi.org/10.1130/0091-7613(1994)022<0247:CTCAEA>2.3.CO;2.

DeCelles, P.G., Ducea, M.N., Kapp, P., and Zandt, G., 2009, Cyclicity in Cordilleran orogenic systems: Nature Geoscience, v. 2, p. 251–257, https://doi.org/10.1038/ngeo469.

DePaolo, D.J., Linn, A.M., and Schubert, G., 1991, The continental crustal age distribution: Methods of determining mantle separation ages from Sm-Nd isotopic data and application to the southwestern United States: Journal of Geophysical Research, v. 96, p. 2071–2088, https://doi.org/10.1029/90JB02219.

Economos, R., Roell, J.L., Barth, A.P., and Wooden, J.L., 2010b, Contrasting sources and construction of Cretaceous granite plutons in the Mojave, CA using whole rock geochemistry and zircon geochronology and geochemistry: Geological Society of America Abstracts with Programs, v. 42, no. 5, p. 666.

Economos, R.C., Barth, A.P., and Wooden, J.L., 2010a, Southern US Cordillera premagmatic zircons: Sounding a Cordilleran source region: Geochimica et Cosmochimica Acta, v. 74, p. 258.

Economos, R.C., Barth, A.P., Wooden, J.L., Howard, K.A., and Wiegand, B.P., 2010c, Comparing batholith-source

connections for the Cadiz Valley Batholith and a deeper sheeted intrusive complex in the Mojave Desert, CA through whole rock and pre-magmatic zircon geochemistry: Eos (Transactions, American Geophysical Union), Fall Meeting Supplement, Paper no. V51E-02.

Economos, R.C., Barth, A.P., Wooden, J.L., Paterson, S.R., Friesenhahn, B., Wiegand, B.A., Anderson, J.L., Roell, J.L., Palmer, E.F., Ianno, A.J., and Howard, K.A., 2021, Testing models of Laramide orogenic initiation by investigation of Late Cretaceous magmatic-tectonic evolution of the central Mojave sector of the California arc: Geosphere, v. 17, p. 2042–2061, https://doi.org/10.1130/GES02225.1.

Engebretson, D.C., Cox, A., and Thompson, G.A., 1984, Correlation of plate motions with continental tectonics: Laramide to basin-range: Tectonics, v. 3, p. 115–119, https://doi.org/10.1029/TC003i002p00115.

Farmer, G.L., Perry, F.V., Semken, S., Crowe, B., Curtis, D., and DePaolo, D.J., 1989, Isotopic evidence on the structure and origin of subcontinental lithospheric mantle in southern Nevada: Journal of Geophysical Research. Solid Earth, v. 94, p. 7885–7898, https://doi.org/10.1029/JB094iB06p07885.

Feuerbach, D.L., Smith, E.I., Walker, J.D., and Tangeman, J.A., 1993, The role of the mantle during crustal extension: Constraints from geochemistry of volcanic rocks in the Lake Mead area, Nevada and Arizona: Geological Society of America Bulletin, v. 105, p. 1561–1575, https://doi.org/10.1130/0016-7606(1993)105<1561:TROTMD>2.3.CO;2.

Feuerbach, D.L., Reagan, M.K., Faulds, J.E., and Walker, J.D., 1998, Lead isotopic evidence for synextensional lithospheric ductile flow in the Colorado River extensional corridor, western United States: Journal of Geophysical Research, v. 103, p. 2515–2528, https://doi.org/10.1029/97JB03210.

Fisher, C.M., Hanchar, J.M., Miller, C.F., Phillips, S., Vervoort, J.D., and Whitehouse, M.J., 2017, Combining Nd isotopes in monazite and Hf isotopes in zircon to understand complex open-system processes in granitic magmas: Geology, v. 45, p. 267–270 https://doi.org/10.1130/G38458.1.

Foster, D.A., Harrison, T.M., and Miller, C.F., 1989, Age, inheritance, and uplift history of the Old Woman–Piute batholith, California, and implications for K-feldspar age spectra: The Journal of Geology, v. 97, p. 232–243, https://doi.org/10.1086/629297.

Fox, L.K., and Miller, D.M., 1990, Jurassic granitoids and related rocks of the southern Bristol Mountains, southern Providence Mountains, and Colton Hills, Mojave Desert, California, *in* Anderson, J.L., ed., The Nature and Origin of Cordilleran Magmatism: Geological Society of America Memoir 174, p. 111–132, https://doi.org/10.1130/MEM174-p111.

Gans, P.B., and Gentry, B.J., 2016, Dike emplacement, footwall rotation, and the transition from magmatic to tectonic extension in the Whipple Mountains metamorphic core complex, southeastern California: Tectonics, v. 35, p. 2564–2608, https://doi.org/10.1002/2016TC004215.

Gaschnig, R.M., Vervoort, J.D., Lewis, R.S., and Tikoff, B., 2011, Isotopic evolution of the Idaho batholith and Challis intrusive province, northern US Cordillera: Journal of Petrology, v. 52, p. 2397–2429, https://doi.org/10.1093/petrology/egr050.

Girardi, J.D., Patchett, P.J., Ducea, M.N., Gehrels, G.E., Cecil, M.R., Rusmore, M.E., Woodsworth, G.J., Pearson, D.M., Manthei, C., and Wermore, P., 2012, Elemental and isotopic evidence for granitoid genesis from deep-seated sources in the Coast Mountains batholith, British Columbia: Journal of Petrology, v. 53, p. 1505–1536, https://doi.org/10.1093/petrology/egs024.

Gerber, M.E., Miller, C.F., and Wooden, J.L., 1995, Plutonism at the eastern edge of the Cordilleran Jurassic magmatic belt, Mojave Desert, California, *in* Miller, D.M., and Busby, C., eds., Jurassic Magmatism and Tectonics of the North American Cordillera: Geological Society of America Special Paper 299, p. 351–374.

Goodge, J.W., and Vervoort, J.D., 2006, Origin of Mesoproterozoic A-type granites in Laurentia; Hf isotope evidence: Earth and Planetary Science Letters, v. 243, p. 711–731, https://doi.org/10.1016/j.epsl.2006.01.040.

Hamilton, W.B., 1969, Mesozoic California and the underflow of the Pacific mantle: Geological Society of America Bulletin, v. 80, p. 2409–2430, https://doi.org/10.1130/0016-7606(1969)80[2409:MCATUO]2.0.CO;2.

Hammond, J.G., 1990, Middle Proterozoic diabase intrusions in the southwestern U.S.A. as indicators of limited extensional tectonism, *in* Gower, C.F., Rivers, T., and Ryan, B., eds., Mid-Proterozoic Laurentia-Baltica: Geological Association of Canada Special Paper 38, p. 517–531.

Hanchar, J.M., Miller, C.F., Wooden, J.L., Bennett, V.C., and Staude, J.-M.G., 1994, Evidence from xenoliths for a dynamic lower crust, eastern Mojave Desert, California: Journal of Petrology, v. 35, p. 1377–1415, https://doi.org/10.1093/petrology/35.5.1377.

Haschke, M.R., Scheuber, E., Gunther, A., and Reutter, K.-J., 2002, Evolutionary cycles during the Andean orogeny: Repeated slab breakoff and flat subduction?: Terra Nova, v. 14, p. 49–55, https://doi.org/10.1046/j.1365-3121.2002.00387.x.

Heller, P.L., and Liu, L.J., 2016, Dynamic topography and vertical motion of the U.S. Rocky Mountain region prior to and during the Laramide orogeny: Geological Society of America Bulletin, v. 128, p. 973–988, https://doi.org/10.1130/B31431.1.

Henderson, L.J., Gordon, R.G., and Engebretson, D.G., 1984, Mesozoic aseismic ridge on the Farallon plate and southward migration of shallow subduction during the Laramide orogeny: Tectonics, v. 3, p. 121–132, https://doi.org/10.1029/TC003i002p00121.

Hildebrand, R.S., and Whalen, J.B., 2017, The Tectonic Setting and Origin of Cretaceous Batholiths within the North American Cordillera: The Case for Slab Failure Magmatism and Its Significance for Crustal Growth: Geological Society of America Special Paper 532, 113 p., https://doi.org/10.1130/2017.2532.

Holland, M.E., Karlstrom, K.E., Gehrels, G., Shufeldt, O.P., Begg, G., Griffin, W., and Belousova, E., 2018, The Paleoproterozoic Vishnu basin in southwestern Laurentia: Implications for supercontinent reconstructions, crustal growth, and the origin of the Mojave crustal province: Precambrian Research, v. 308, p. 1–17, https://doi.org/10.1016/j.precamres.2018.02.001.

Howard, K.A., 1993, Volcanic history of the Colorado River extensional corridor: Active or passive rifting?: Geological Society of America Abstracts with Programs, v. 25, no. 5, p. 54.

Howard, K.A., 2002, Geologic map of the Sheep Hole Mountains 30′ x 60′ quadrangle, San Bernardino and Riverside Counties, California: U.S. Geological Survey map MF-2344, 2 sheets, http://pubs.usgs.gov/mf/2002/2344/, scale 1:100,000.

Howard, K.A., and John, B.E., 1987, Crustal extension along a rooted system of imbricate low-angle faults: Colorado River extensional corridor, California and Arizona, *in* Coward, M.P., Dewey, J.F., and Hancock, P.L., eds., Continental Extensional Tectonics: Geological Society of London Special Publication 28, p. 299–311.

Howard, K.A., McCaffrey, K.J.W., Wooden, J.L., Foster, D.A., and Shaw, S.E., 1995, Jurassic thrusting of Precambrian basement over Paleozoic cover in the Clipper Mountains, southeastern California, *in* Miller, D.M., and Busby, C., eds., Jurassic Magmatism and Tectonics of the North American Cordillera: Geological Society of America Special Paper 299, p. 375–392, https://doi.org/10.1130/SPE299-p375.

Howard, K.A., John, B.E., Nielson, J.E., Miller, J.M.G., and Wooden, J.L., 2013, Geologic map of the Topock 7.5-minute quadrangle, Arizona and California: U.S. Geological Survey Scientific Investigations Map SIM-3236 (1:24,000), with pamphlet, 60 p., http://pubs.usgs.gov/sim/3236/.

Howard, K.A., Shaw, S.E., Allen, C.M., and Pearson, N.J., 2016, Mesozoic and Tertiary pluton sources in Mojave continental crust—Zircon U-Pb and Lu-Hf isotopic evidence: Geological Society of America, Cordilleran Section Meeting Program, v. 48, no. 4, presentation 13-5 https://gsa.confex.com/gsa/2016CD/webprogram/Paper274508.html.

John, B.E., and Foster, D.A., 1993, Structural and thermal constraints on the initiation angle of detachment faulting in the southern Basin and Range: The Chemhuevi Mountains case study: Geological Society of America Bulletin, v. 105, p. 1091–1108, https://doi.org/10.1130/0016-7606(1993)105<1091:SATCOT>2.3.CO;2.

Jones, R.E., Kirstein, L.A., Kasemann, S.A., Dhuime, B., Elliott, T., Litvak, V.D., Alonso, R., Hinton, R., and Facility, E.I.M., 2015, Geodynamic controls on the contamination of Cenozoic arc magmas in the southern Central Andes: Insights from the O and Hf isotopic composition of zircon: Geochimica et Cosmochimica Acta, v. 164, p. 386–402, https://doi.org/10.1016/j.gca.2015.05.007.

Kapp, J.D., Miller, C.F., and Miller, J.S., 2002, Ireteba pluton, Eldorado Mountains, Nevada: Late, deep-source, peraluminous magmatism in the Cordilleran interior: The Journal of Geology, v. 110, p. 649–669, https://doi.org/10.1086/342864.

Kemp, A.I.S., Hawkesworth, C.J., Collins, W.J., Gray, C.M., Blevin, P.L., and EIMF, 2009, Isotopic evidence for rapid continental growth in an extensional accretionary orogeny: The Tasmanides, eastern Australia: Earth and Planetary Science Letters, v. 284, p. 455–466, https://doi.org/10.1016/j.epsl.2009.05.011.

Klemetti, E.W., Lackey, J.S., and Starnes, J., 2014, Magmatic lulls in the Sierra Nevada captured in zircon from rhyolite of the Mineral King pendant, California: Geosphere, v. 10, no. 1, p. 66–79 https://doi.org/10.1130/GES00920.1.

Kula, J.L., Spell, T.L., and Wells, M.L., 2002, Syntectonic intrusion and exhumation of a Mesozoic plutonic complex in the Late Cretaceous, Granite Mountains, southeastern California: Geological Society of America Abstracts with Programs, v. 34, no. 6, p. 249.

LaForge, J.S., John, B.E., and Grimes, C.B., 2017, Synextensional dike emplacement across the footwall of a continental core complex, Chemehuevi Mountains, southeastern California: Geosphere, v. 13, p. 1867–1886, https://doi.org/10.1130/GES01402.1.

Lee, C.-T., Yin, Q., Rudnick, R.L., and Jacobsen, S.B., 2001, Preservation of ancient and fertile lithospheric mantle beneath the southwestern United States: Nature, v. 411, p. 69–73, https://doi.org/10.1038/35075048.

Leventhal, J.A., Reid, M.R., Montana, A., and Holden, P., 1995, Mesozoic invasion of crust by MORB-source asthenospheric magmas, U.S. Cordilleran interior: Geology, v. 23, p. 399–402 https://doi.org/10.1130/0091-7613(1995)023<0399:MIOCBM>2.3.CO;2.

Liu, L., Gurnis, M., Seton, M., Saleeby, J., Müller, R.D., and Jackson, J.M., 2010, The role of oceanic plateau subduction in the Laramide orogeny: Nature Geoscience, v. 33, p. 353–357, https://doi.org/10.1038/NGEO829.

Luffi, P., Saleeby, J.B., Lee, C.A., and Ducea, M.N., 2009, Lithospheric mantle duplex beneath the central Mojave Desert revealed by xenoliths from Dish Hill, California: Journal of Geophysical Research, v. 114, https://doi.org/10.1029/2008JB005906.

Mamani, M., Wörner, G., and Sempere, T., 2010, Geochemical variations in igneous rocks of the Central Andean orocline (13°S to 18°S): Tracing crustal thickening and magma generation through time and space: Geological Society of America Bulletin, v. 122, p. 162–182, https://doi.org/10.1130/B26538.1.

McDowell, S.M., Overton, S., Fisher, C.M., Frazier, W.O., Miller, C.F., Miller, J.S., and Economos, R.C., 2016, Hafnium, oxygen, neodymium, strontium, and lead isotopic constraints on magmatic evolution of the supereruptive southern Black Mountains volcanic center, Arizona, U.S.A.: A combined LASS zircon–whole-rock study: The American Mineralogist, v. 101, p. 311–327 https://doi.org/10.2138/am-2016-5127.

Mendoza, O.T., and Suastegui, M.G., 2000, Geochemistry and isotopic composition of the Guerrero Terrane (western Mexico): Implications for the tectonomagmatic evolution of southwestern North America during the late Mesozoic: Journal of South American Earth Sciences, v. 13, p. 297–324, https://doi.org/10.1016/S0895-9811(00)00026-2.

Miller, C.F., and Barton, M.D., 1990, Phanerozoic plutonism in the Cordilleran interior, USA, *in* Kay, M.S., and Rapela, C.W., eds., Plutonism from Antarctica to Alaska: Geological Society of America Special Paper 241, p. 213–231, https://doi.org/10.1130/SPE241-p213.

Miller, C.F., and Wooden, J.L., 1994, Anatexis, hybridization and the modification of ancient crust: Mesozoic plutonism in the Old Woman Mountains area, California: Lithos, v. 32, p. 111–133, https://doi.org/10.1016/0024-4937(94)90025-6.

Miller, C.F., Wooden, J.L., Bennett, V.C., Wright, J.E., Solomon, G.C., and Hurst, R.W., 1990, Petrogenesis of the composite peraluminous-metaluminous Old Woman–Piute Range batholith, southeastern California: isotopic constraints, *in* Anderson, J.L., ed., The Nature and Origin of Cordilleran Magmatism: Geological Society of America Memoir 174, p. 99–110, https://doi.org/10.1130/MEM174-p99.

Miller, C.F., Hanchar, J.M., Wooden, J.L., Bennet, V.C., Harrison, T.M., Wark, D.A., and Foster, D.A., 1992, Source region of a granite batholith; Evidence from lower crustal xenoliths and inherited accessory minerals: Royal Society of Edinburgh, Earth Science: Transactions, v. 83, p. 49–62.

Miller, C.F., McDowell, S.M., and Mapes, R.W., 2003, Hot and cold granites?: Implications of zircon saturation temperatures and preservation of inheritance: Geology, v. 31, p. 529–532, https://doi.org/10.1130/0091-7613(2003)031<0529:HACGIO>2.0.CO;2.

Miller, J.S., and Glazner, A.G., 1995, Jurassic plutonism and crustal evolution in the central Mojave Desert, California: Contributions to Mineralogy and Petrology, v. 118, p. 379–395, https://doi.org/10.1007/s004100050021.

Miller, J.S., Glazner, A.F., Farmer, A.L., Suayay, I.B., and Keith, L.A., 2000, A Sr, Nd, and Pb isotopic study of mantle domains and crustal structure from Miocene volcanic rocks in the Mojave Desert, California: Geological Society of America Bulletin, v. 112, p. 1264–1279, https://doi.org/10.1130/0016-7606(2000)112<1264:ASNAPI>2.0.CO;2.

Miller, J.S., Walker, B.A., Miller, C.F., Claiborne, L.L., Davies, G.R., and Wooden, J.L., 2009, Growth of the Spirit Mountain batholith (Nevada, USA) as revealed by in situ Hf isotopes in zircon: Geological Society of America Abstracts with Programs, v. 41, no. 7, p. 60 https://gsa.confex.com/gsa/2009AM/webprogram/Paper166969.html.

Nelson, D.A., and Cottle, J.M., 2018, The secular development of accretionary orogens: Linking the Gondwana magmatic arc record of West Antarctica, Australia, and South America: Gondwana Research, v. 63, p. 15–33, https://doi.org/10.1016/j.gr.2018.06.002.

Pease, V., Foster, D., Wooden, J., O'Sullivan, P., Argent, J., and Fanning, C., 1999, The northern Sacramento Mountains, southwest United States. Part II: Exhumation history and detachment faulting, *in* MacNiocaill, C., and Ryan, P.D., eds., Continental Tectonics: Geological Society of London Special Publication 164, p. 199–237.

Pease, V., Hillhouse, J.W., and Wells, R.E., 2005, Paleomagnetic quantification of upper-plate deformation during Miocene detachment faulting in the Mohave Mountains, Arizona: Geochemistry, Geophysics, Geosystems, v. 6, no. 9, https://doi.org/10.1029/2005GC000972.

Pepper, M., Gehrels, G., Pullen, A., Ibanez-Mejia, M., Ward, K.M., and Kapp, P., 2016, Magmatic history and crustal genesis of western South America: Constraints from U-Pb ages and Hf isotopes of detrital zircons in modern rivers: Geosphere, v. 12, p. 1532–1555, https://doi.org/10.1130/GES01315.1.

Phillips, S.E., Hanchar, J.M., Miller, C.F., Fisher, C.M., Lancaster, P.J., and Darling, J.R., 2014, High spatial-resolution isotope geochemistry of monazite (U-Pb & Sm-Nd) and zircon (U-Pb and Lu-Hf) in the Old Woman Piute Range batholith, Mojave Desert, California: Geological Society of America, Abstracts with Programs, v. 46, no. 6, p. 548, https://gsa.confex.com/gsa/2014AM/webprogram/Paper246107.html.

Piercey, S.J., Mortensen, J.K., and Creaser, R.A., 2003, Neodymium isotope geochemistry of felsic volcanic and intrusive rocks from the Yukon-Tanana Terrane in the Finlason Lake region, Yukon, Canada: Canadian Journal of Earth Sciences, v. 40, p. 77–97, https://doi.org/10.1139/e02-094.

Poole, G.H., Kemp, I.S., Hagemann, S.G., Fiorentini, H.J., Jeon, H., Williams, I.S., Zappettini, E.O., and Rubenstein, N.A., 2020, The petrogenesis of back-arc magmas, constrained by zircon O and Hf isotopes, in the frontal Cordillera and Precordillera, Argentina: Contributions to Mineralogy and Petrology, v. 175, p. 89, https://doi.org/10.1007/s00410-020-01721-0.

Profeta, L., Ducea, M.N., Chapman, J.B., Paterson, S.R., Gonzalez, S.M., Kirsch, M., Petrescu, L., and DeCelles, P.G., 2015, Quantifying crustal thickness over time in magmatic arcs: Scientific Reports, v. 5, https://doi.org/10.1038/srep17786.

Rämö, O.T., and Calzia, J.P., 1998, Nd isotopic composition of cratonic rocks in the southern Death Valley region: Evidence for a substantial Archean source component in Mojavia: Geology, v. 26, p. 891–894, https://doi.org/10.1130/0091-7613(1998)026<0891:NICOCR>2.3.CO;2.

Rämö, O.T., Calzia, J.P., and Kosunen, P.L., 2002, Geochemistry of Mesozoic plutons, southern Death Valley region, California: Insights into the origin of Cordilleran interior magmatism: Contributions to Mineralogy and Petrology, v. 143, p. 416–437, https://doi.org/10.1007/s00410-002-0354-9.

Ryan, M., 2011, Mixing and melt sources in the Miocene Aztec Wash pluton (Nevada, USA) as revealed by zircon Hf and O and whole rock Sr, Nd, and Hf isotopes [M.S. thesis]: San Jose, California, San Jose State University, 395 p.

Saleeby, J., 2003, Segmentation of the Laramide slab—Evidence from the southern Sierra Nevada region: Geological Society of America Bulletin, v. 115, p. 655–668, https://doi.org/10.1130/0016-7606(2003)115<0655:SOTLSF>2.0.CO;2.

Shaw, S.E., Flood, R.H., and Pearson, N.J., 2011, The New England Batholith of eastern Australia: Evidence of silicic magma mixing from zircon $^{176}Hf/^{177}Hf$ ratios: Lithos, v. 126, p. 115–126, https://doi.org/10.1016/j.lithos.2011.06.011.

Shaw, S.E., Todd, V.R., Kimbrough, D.L., and Pearson, N.J., 2014, A west-to-east transect across the Peninsular Ranges batholith, San Diego County, California: Zircon $^{176}Hf/^{177}Hf$ evidence for the mixing of crustal- and mantle-derived magmas, and comparisons with the Sierra Nevada batholith, *in* Morton, D.M., and Miller, F.K., eds., Peninsular Ranges Batholith, Baja California and Southern California: Geological Society of America Memoir 211, p. 499–536, https://doi.org/10.1130/2014.1211(15).

Siégel, C., Bryan, S.E., Allen, C.M., Gust, D.A., and Purdy, D.J., 2020, Crustal evolution in the New England orogen, Australia: Repeated igneous activity and scale of magmatism govern the composition and isotopic character of the continental crust: Journal of Petrology, v. 61, no. 8, p. 1–28, https://doi.org/10.1093/petrology/egaa078.

Strickland, E.D., Singleton, J.S., and Haxel, G.B., 2018, Orocopia Schist in the northern Plomosa Mountains, west-central Arizona: A Laramide subduction complex exhumed in a Miocene metamorphic core complex: Lithosphere, v. 10, p. 723–742, https://doi.org/10.1130/L742.1.

Tatsumi, Y., 2005, The subduction factory: How it operates in the evolving Earth: GSA Today, v. 15, no. 7, p. 4–10,https://doi.org/10:1130/1052-5173(2005)015<4:TSFHIO>2.0.CO;2.

Timmermans, A.C., Cousens, B.L., and Henry, C.D., 2020, Geochemical study of Cenozoic mafic volcanism in the west-central Great Basin, western Nevada, and the ancestral Cascades arc, California: Geosphere, v. 16, no. 5, p. 1179–1207, https://doi.org/10.1130/GES01535.1.

Tosdal, R.M., and Wooden, J.L., 2015, Construction of the Jurassic magmatic arc, southeast California and southwest Arizona, *in* Anderson, T.H., ed., Late Jurassic margin of Laurasia—A record of faulting accommodating plate rotation: Geological Society of America Special Paper 513, p. 189–221, https://doi.org/10.1130/2015.2513(04).

Tosdal, R.M., Haxel, G.B., and Wright, J.E., 1989, Jurassic geology of the Sonoran Desert region, southernmost Arizona, southeastern California, and northernmost Sonora: Arizona Geological Society Digest, v. 17, p. 397–434.

Vermeesch, P., 2018, IsoplotR: A free and open toolbox for geochronology: Geoscience Frontiers, v. 9, p. 1479–1493, https://doi.org/10.1016/j.gsf.2018.04.001.

Walker, J.D., Martin, M.W., Glazner, A.F., and Bartley, J.M., 2002. Late Paleozoic to Mesozoic development of the Mojave Desert and environs, California, *in* Glazner, A.F., Walker, J.D., and

Bartley, J.M., eds., Geologic Evolution of the Mojave Desert and Southwestern Basin and Range: Geological Society of America Memoir 195, p.1–18, https://doi.org/10.1130/0-8137-1195-9.1.

Ward, P.W., 1991, On plate tectonics and the geologic evolution of southwestern North America: Journal of Geophysical Research, v. 96, p. 12,479–12,496, https://doi.org/10.1029/91JB00606.

Wells, M.L., and Hoisch, T.D., 2008, The role of mantle delamination in widespread Late Cretaceous extension and magmatism in the Cordilleran orogen, western United States: Geological Society of America Bulletin, v. 120, p. 515–530, https://doi.org/10.1130/B26006.1.

Wells, M.L., Spell,T.L., and Grove, M. , 2002, Late Cretaceous intrusion and extensional exhumation of the Cadiz Valley batholith, Iron Mountains, southeastern California: Geological Society of America Abstracts with Programs, v. 34, no. 79–5, p. 178.

Wooden, J.L., and DeWitt, E., 1991, Pb isotopic evidence for the boundary between the Early Proterozoic Mojave and central Arizona crustal provinces in western Arizona: Arizona Geological Digest, v. 19, p. 27–50.

Wooden, J.L., and Miller, D.M., 1990, Chronologic and isotopic framework for Early Proterozoic crustal evolution in the eastern Mojave Desert region, SE California: Journal of Geophysical Research, v. 95, p. 20,133–20,146, https://doi.org/10.1029/JB095iB12p20133.

Wooden, J.L., Stacey, J.S., Howard, K.A., Doe, B.R., and Miller, D.M., 1988, Pb isotopic evidence for the formation of Proterozoic crust in the southwestern United States, *in* Ernst, W.G., ed., Metamorphism and crustal evolution of the western United States, Rubey Volume VII: Englewood Cliffs, New Jersey, Prentice-Hall, p. 69–86.

Wooden, J.L., Barth, A.P., and Mueller, P.A., 2013, Crustal growth and tectonic evolution of the Mojave crustal Province: Insights from hafnium isotope systematics in zircons: Lithosphere, v. 5, p. 17–28, https://doi.org/10.1130/L218.1.

Wooden, J.L., Barth, A.P., Mueller, P.A., Miller, D.M., and Howard, K.A., 2017a, Hf isotopic record of magmatic secular variation in the Cordilleran continental arc in southern California: Geological Society of America Abstracts with Programs, v. 49, no. 4, https://doi.org/10.1130/abs/2017CD-292330.

Wooden, J.L., Wright, J.E., Howard, K.A., Barth, A.P., and Anderson, J.L., 2017b, Implications of new SIMS zircon ages for magmatic evolution of the Whipple Mountains metamorphic core complex: Geological Society of America Abstracts with Programs, v. 49, no. 6, https://doi.org/10.1130/abs/2017AM-299472.

Wright, J.E., Howard, K.A., and Anderson, J.L., 1987, Isotopic systematics of zircons from Late Cretaceous intrusive rocks, southeastern California: Implications for a vertically stratified crustal column: Geological Society of America Abstracts with Programs, v. 19, no. 7, p. 898.

Young, E.D., Wooden, J.L., Shieh, Y.N., and Farber, D., 1992, Geochemical evolution of Jurassic diorites from the Bristol Lake region, California, USA, and the role of assimilation: Contributions to Mineralogy and Petrology, v. 110, p. 68–86 https://doi.org/10.1007/BF00310883.